CAPITAL UNIVERSITY OF SCIENCE AND TECHNOLOGY, ISLAMABAD

Transfersomal Gel as a Nanocarrier Platform for Enhanced Delivery and Efficacy of Silver Sulphadiazine

by

Muneeba Basharat

A thesis submitted in partial fulfillment for the degree of Master of Philosophy

in the

Faculty of Pharmacy
Department of Pharmaceutics

2026

CERTIFICATE OF APPROVAL

Transfersomal Gel as a Nanocarrier Platform for Enhanced Delivery and Efficacy of Silver Sulphadiazine

by

Muneeba Basharat

(Registration No: MPH243013)

THESIS EXAMINING COMMITTEE

S. No.	Examiner	Name	Organization
(a)	External Examiner	Dr. Maria Mir	Iqra Uni., Islamabad
(b)	Internal Examiner	Dr. Fazlullah Khan	CUST, Islamabad

Dr Mahira Zeeshan
Thesis Supervisor
September, 2026

Dr Nadia Shamshad Malik
Head
Dept. of Pharmaceutics
September, 2026

Dr. Muzaffar Abbas
Dean
Faculty of Pharmacy
September, 2026

Author's Declaration

I, **Muneeba Basharat** hereby state that my MPhil thesis titled "**Transfersomal Gel as a Nanocarrier Platform for Enhanced Delivery and Efficacy of Silver Sulphadiazine**" is my own work and has not been submitted previously by me for taking any degree from Capital University of Science and Technology, Islamabad or anywhere else in the country/abroad.

At any time if my statement is found to be incorrect even after my graduation, the University has the right to withdraw my MPhil Degree.

(Muneeba Basharat)

Registration No: MPH243013

Plagiarism Undertaking

I solemnly declare that research work presented in this thesis titled "**Transfersomal Gel as a Nanocarrier Platform for Enhanced Delivery and Efficacy of Silver Sulphadiazine**" is solely my research work with no significant contribution from any other person. Small contribution/help wherever taken has been duly acknowledged and that complete thesis has been written by me.

I understand the zero tolerance policy of the HEC and Capital University of Science and Technology towards plagiarism. Therefore, I as an author of the above titled thesis declare that no portion of my thesis has been plagiarized and any material used as reference is properly referred/cited.

I undertake that if I am found guilty of any formal plagiarism in the above titled thesis even after award of MPhil Degree, the University reserves the right to withdraw/revoke my MPhil degree and that HEC and the University have the right to publish my name on the HEC/University website on which names of students are placed who submitted plagiarized work.

(Muneeba Basharat)

Registration No: MPH243013

Acknowledgement

First and foremost, all praise and gratitude are due to **Almighty Allah (SWT)**, the Most Gracious and the Most Merciful, whose infinite blessings, mercy, and guidance granted me the strength, patience, wisdom, and perseverance to complete this research successfully. Without His countless favors and divine support, this accomplishment would not have been possible.

I would like to express my deepest gratitude and sincere appreciation to my research supervisor, **Dr. Mahira Zeeshan**, for her invaluable guidance, continuous encouragement, and unwavering support throughout this research. Her remarkable knowledge and insightful suggestions inspired me to approach scientific research with confidence and dedication.

I would also like to express my sincere gratitude to **Dr. Nadia Shamshad Malik**, whose exceptional mentorship, expert guidance, thoughtful suggestions, continuous encouragement, and valuable advice greatly enriched this research.

My heartfelt gratitude goes to my **parents**, whose endless sacrifices, unwavering faith, and continuous prayers have been the greatest source of strength throughout my life. From my childhood, they have always encouraged me to pursue knowledge with determination and integrity. Their patience, understanding, and unwavering belief in my abilities made this journey easier.

I wish to express my deepest and special appreciation to my husband, **Umar Farooq**. His unwavering support, patience, encouragement, understanding, and constant belief in me gave me the confidence to overcome every challenge. He stood beside me from the very beginning, offering not only emotional strength but also countless hours of practical assistance during the writing, reviewing, and organization of the thesis. His thoughtful discussions, continuous motivation, and willingness to share my academic responsibilities transformed difficult moments into manageable ones. His steadfast companionship has been invaluable, and his unwavering support made this challenging journey truly memorable.

I would also like to express my sincere gratitude to my family member, Tahir Raza of Fudan University, China, for his invaluable support during the key laboratory analyses conducted at Fudan University. My heartfelt appreciation also goes to my siblings, friends, and colleagues, whose encouragement, kindness, and positivity made this journey more enjoyable and memorable.

Finally, I gratefully acknowledge the Department of Pharmacy, Capital University of Science and Technology (CUST), Islamabad, and all faculty members and laboratory staff for providing an excellent academic environment, modern research facilities, and the necessary resources that made this work possible.

(Muneeba Basharat)

Abstract

Wound infections remain a persistent challenge in clinical practice, often resulting in delayed healing, frequent dressing changes, limited penetration of conventional topical drugs, and growing concern about antimicrobial resistance. Although silver sulphadiazine (SSD) has long been regarded as an effective topical antimicrobial agent, its therapeutic performance is restricted by poor skin penetration and the need for repeated application. To overcome these limitations, the present study focused on the development of SSD-loaded transfersomes (SSD-TFs) coloaded into chitosan gel to form SSD-loaded transfersomal chitosan gel (SSD-TFs-Chi gel). The SSD-TFs-Chi gel was designed to enhance drug delivery into the skin, provide sustained drug release, prolong drug retention, and improve antibacterial efficacy while maintaining dermal safety.

SSD-TFs were prepared successfully using the thin-film hydration method and optimized to produce nanosized vesicles with high drug entrapment efficiency, favorable physicochemical characteristics, and good colloidal stability. The nanoformulation was characterized by evaluating vesicle size, polydispersity index, zeta potential, entrapment efficiency, compatibility between drug and excipients using Attenuated Total Reflectance Fourier-transform infrared spectroscopy (ATR-FTIR), physical form of drug inside SSD-TFs using X-ray powder diffraction (XPRD), and morphology using field emission transmission electron microscopy (FE-TEM). Further, drug release from SSD-TFs was explored at pH 5.5 and 7.4, and drug release kinetics were evaluated to study the mechanism of drug release. Afterwards, SSD-TFs were incorporated into a chitosan-based gel to produce SSD-TFs-Chi gel. The SSD-TFs-Chi gel was evaluated for pH, spreadability, viscosity, physical stability, and permeability. FE-TEM analysis revealed predominantly spherical and uniformly distributed nanovesicles with minimal aggregation. ATR-FTIR findings confirmed the absence of chemical incompatibility among the formulation components, while XPRD analysis demonstrated a conversion of the crystalline nature of silver sulphadiazine into an amorphous form because of its

encapsulation within the transfersomal vesicles, indicating successful incorporation into the nanocarrier system. Furthermore, stability studies conducted under refrigerated, ambient, and accelerated storage conditions demonstrated that the formulation remained physically stable with no significant changes in appearance, homogeneity, and pH throughout the study period.

The optimized SSD-TFs-Chi gel demonstrated significantly greater and more sustained drug release than the conventional formulation at both pH 5.5 and 7.4, with release predominantly governed by diffusion. The Higuchi and Korsmeyer–Peppas models best described release at pH 7.4, while the Korsmeyer–Peppas model provided the best fit at pH 5.5, indicating predominantly Fickian diffusion. Ex vivo permeation studies further showed that the deformable transfersomal vesicles enhanced passage across the stratum corneum, resulting in prolonged skin drug retention and an approximately two-fold increase in permeation with SSD-TFs-Chi gel. The enhanced delivery resulted in greater antibacterial activity against Staphylococcus aureus, as evidenced by larger zones of inhibition than the conventional formulation. In vivo skin irritation and histopathological studies demonstrated negligible erythema and edema with preserved normal skin architecture, confirming the formulation's dermal biocompatibility and safety.

Overall, this study demonstrates that SSD-TFs-Chi gel effectively addresses several shortcomings with conventional topical therapy and offers a promising nanovesicular platform for topical drug delivery.

Contents

List of Figures

List of Tables

Abbreviations

ATR-FTIR	Attenuated Total Reflectance Fourier Transform Infrared Spectroscopy
Chi gel	Chitosan gel
DMSO	Dimethyl sulfoxide
EA	Edge Activator
ECM	Extracellular matrix
EGF	Epidermal growth factor
FE-TEM	Field Emission Transmission Electron Microscopy
H & E	Hematoxylin and Eosin
HPMC	Hydroxypropyl methylcellulose
MHA	Mueller–Hinton agar
PBS	Phosphate Buffer Solution
PDI	Polydispersity Index
PDGF	Platelet-derived growth factor
P. aeruginosa	Pseudomonas aeruginosa
S. aureus	Staphylococcus aureus
SC	Stratum corneum
SSD	Silver Sulphadiazine
SSD-Tfs	Silver Sulphadiazine-Loaded Transfersomes
SSD-Tfs Chi	Silver Sulphadiazine Transfersomal Chitosan
TBSA	Total Body Surface Area
Tfs	Transfersomes
TGF	Transforming Growth Factor
ZOI	Zone of Inhibition

Chapter 1

Introduction

1.1 Background

The Skin serves as considered the largest organ in the human organism, with area of surface roughly two square meters in the average individual adult. Dermis and Epidermis are key parts of skin, which hold essentials skin appendage structures, such as sweat glands, sebaceous glands, and hair follicles [1]. The primary skin function is to create a strong protective interface between the body's "inside" and "outside". The chemical and biochemical antimicrobial and innate immune systems, physical barriers, and adaptive immunological defense system are all components of the epidermis. The principal physical barrier of the skin is formed by the stratum corneum (SC), whereas the underlying nucleated epidermis contributes to barrier function through intercellular junctions and cytoskeletal protein networks. Lipids, acids, hydrolytic enzymes, antimicrobial peptides, and macrophages are biochemical. The humoral and cellular components of the immune system make up the immunological barrier [2].

Burn injuries are among the most severe forms of traumatic injury affecting the integumentary system and lead to impose a significant clinical, societal, and economic burden on healthcare systems worldwide.

Although considerable progress has been made in critical care, surgical intervention, and infection control strategies, burn-associated morbidity and mortality continue to remain alarmingly high, particularly in countries having low and middle-income. Burns comes under the health issue of general public at globe, resulting in an estimated 180, 000 casualties each year [3]. In 2016, in the United States, approximately 486,000 individuals sustained burn injuries, reflecting the significant public health burden associated with thermal trauma. Although many cases were managed in outpatient settings, nearly 40,000 patients required hospitalization for specialized treatment, and approximately 75% needed care in dedicated burn centres, highlighting the severity and complexity of moderate to major burn injuries [4]. Burn injuries may result from exposure of the skin to thermal agents such as flames, hot objects, flash burns, scalding liquids, chemicals, grease, or electrical sources. [5]. Burn injuries can vary, and the extent of body surface area involved is a major determinant of wound severity, morbidity, and patient mortality. Severe burns induce not only cutaneous damage but also immune dysfunction and hypermetabolism, collectively contributing to poor clinical outcomes [6].

Burn injuries are classified based on depth, extent, and cause, which is essential for guiding management and predicting outcomes. Superficial burns involve only the epidermis, presenting as red, painful, dry skin without blisters, and typically heal within 3–7 days without scarring. Partial thickness burns extend into the dermis and are subdivided into superficial, characterized by blisters and intense pain, and deep, which appear white or red, may be less painful, and often require grafting. Full-thickness burns destroy the entire dermis and sometimes subcutaneous tissue, with a leathery or charred appearance, usually necessitating surgical intervention. Burn severity is also assessed using total body surface area (TBSA). Burns can result from thermal, chemical, electrical, or radiation sources, and classification by cause helps in determining specific therapeutic strategies [7].

Burn wound restorative is a convoluted and highly coordinated biological technique that progresses through four sequential phases.

Phases: 1. Hemostasis, 2. Inflammation, 3. Proliferation, 4. Remodeling

1.1.1 Hemostasis

Right after injury, hemostasis limits blood loss through vasoconstriction and clot formation, establishing a provisional matrix for repair. This initial phase begins immediately after injury and is characterized by rapid vasoconstriction to minimize blood loss. Platelet activation and aggregation are triggered by exposure to collagen, leading to clot formation.

Activated platelets, together with keratinocytes, macrophages, and fibroblasts, release key multiplier factors such as platelet-derived growth factor (PDGF), epidermal growth factor (EGF), and transforming growth factor (TGF).

These signaling molecules facilitate the development of clot named fibrin at the injury site, creating a provisional extracellular matrix that offers mechanical support and serves as a stage for the subsequent stages of tissue repair [8].

1.1.2 Inflammation

The inflammatory stage is marked by the activation of cells linked with immunity, like the release of proteins (pro-inflammatory cytokines), and the elimination of necrotic tissue. This stage typically begins within the first twenty-four (24) hours after injury and may persist for several days or even weeks, depending on the burn's extent and severity.

It is marked by the activation and mobilization of cells linked with immunity to the site of wound, which trigger the production of proteins (pro-inflammatory cytokines and chemokines). These mediators regulate migration, proliferation, and subsequent activation of epithelial cells, endothelial cells, and fibroblasts, thereby promoting collagen synthesis and tissue remodelling.

Concurrently, necrotic tissue and cellular debris are cleared through phagocytic activity, initiating a cascade of signalling events essential for effective wound repair and progression to the proliferative phase [8].

1.1.3 Proliferation

During proliferation, fibroblast activity, collagen deposition, angiogenesis, and epithelialization restore tissue integrity. During the final remodeling stage, the extracellular matrix undergoes continuous reorganization while collagen fibers mature, leading to improved tensile strength and ultimately influencing the characteristics of the mature scar. The proliferative stage subsequently begins and is characterized by the activity of anti-inflammatory mediators, including IL-4, IL-10, and TGF, which facilitate tissue regeneration and healing [9].

Keratinocytes, which are actively dividing epithelial cells that move toward the fibrin clot and wound bed to restore tissue continuity, are derived from these deep structures and are crucial to the wound-healing process [1].

1.1.4 Remodelling

Finally, during remodelling, growth factors and matrix metalloproteinases regulate scar formation through collagen deposition and fibroblast transformation into myofibroblasts [9]. The remodelling phase generally begins approximately three following injury and can extend beyond twelve months, depending on wound severity and patient-related factors.

At this point of stage, the inflammatory and proliferative activities gradually subside, and many previously activated cells, including macrophages, excess endothelial cells and myofibroblasts either undergo programmed cell death or leave the wound environment as healing progresses. Consequent process results in a scar tissue matrix predominantly consisting predominantly of collagen together with other extracellular matrix (ECM) components.

Dynamic interactions between the epidermis and dermis, along with regulatory feedback mechanisms, contribute to the restoration of skin integrity and structural stability. Over a period of 6–12 months, type III collagen within the ECM is progressively gradually transitions to mechanically stronger and more highly

structured collagen of type I, thereby improving the tensile strength of the repaired tissue and maturation of the scar [10].

The skin functions as a primary mechanical and immunological barrier against microbial invasion. Disruption of this barrier following burn trauma creates a protein-rich, moist environment conducive to microbial colonization. Within 24–48 hours, burn wounds become colonized by endogenous flora, followed by opportunistic nosocomial pathogens [11]. Clinically, local infection presents with increased exudate, purulent discharge, graft loss, cellulitis, and delayed epithelialization, often associated with biofilm-forming pathogens.

If untreated, local infection may progress to systemic infection and septic shock, contributing to 42–65% of burn-related deaths, depending on burn severity [12]. Burn wounds are initially sterile immediately after thermal injury, but this sterile state is short-lived due to rapid microbial colonization by the endogenous microbiota, the hospital environment, and invasive medical devices. The protein-rich, avascular nature of burn tissue provides an ideal environment for rapid bacterial proliferation. Colonization may progress to infection when the microbial load increases and host immune defenses are compromised. Over time, Gram-positive organisms are replaced by Gram-negative and multidrug-resistant pathogens, significantly complicating treatment. Understanding this transition is crucial for preventing invasive infection, sepsis, and burn-related mortality [13].

The microbial spectrum evolves with Gram-positive organisms such as Staphylococcus aureus (S. aureus) predominating in the early phase, followed by Gram-negative bacteria, and later by fungal pathogens and multidrug-resistant organisms. Recognition of this chronological shift is essential for appropriate empirical therapy and infection control in burn patients [4]. Gram-negative organisms are responsible for most infections associated with burn wounds, demonstrating comparable incidence and distribution patterns across different geographic regions and healthcare settings. The Gram-positive pathogen S. aureus, including resistant strains, has been identified as an independent risk factor associated with increased mortality among individuals with burn injuries [14].

TABLE 1.1: Common Wound Infections

Category	**Representative Organism**
Gram-Positive Bacteria	S. aureus
Gram-Negative Bacteria (Early)	Escherichia coli, Klebsiella pneumoniae
Gram-Negative bacteria (late)	P. aeruginosa, Acinetobacter baumannii, Enterobacter cloacae

Infection not only delays the healing process but also increases scarring, necessitates greater use of antibiotics, and substantially raises treatment costs. Bacterial colonization of wounds begins almost immediately after injury, often involving opportunistic pathogens from the patient's own microbiome or the surrounding environment. In many cases, microbial populations remain at low levels that do not significantly interfere with healing. However, in some wounds, microbial proliferation can surpass the immune system's capacity to control it, disrupting normal repair processes and leading to invasive infection that requires targeted medical intervention [15].

To combat these challenges, there is an urgent need for an effective antimicrobial agent that not only prevents infection but also accelerates the wound healing process [16]. Topical antimicrobial therapy remains a mainstay in wound care because it targets pathogens directly at the site of injury, reduces systemic exposure, and can limit the progression of local colonization to invasive infection.

Conventional topical agents include antiseptics, antibiotics, and heavy metal compounds, all designed to suppress bacterial proliferation and prevent wound deepening. Additional agents such as cerium nitrate, often combined with silver sulphadiazine, chlorhexidine, cadexomer iodine, polyhexanide, octenidine dihydrochloride,

nitrofuran, and sodium fusidate contribute to infection control through microbicidal action, wound cleansing, and, in some cases, stimulation of tissue regeneration [17].

Silver and its derivatives have been utilized for centuries as antimicrobial agents. Among them, Silver Sulphadiazine (SSD) remains the most widely used and clinically significant silver-based antibiotic and is the most commonly used topical agent in burn infection management due to its broad-spectrum activity against both Gram-positive and Gram-negative organisms, including S. aureus and Pseudomonas aeruginosa (P. aeruginosa), and is recommended particularly for deep partial and full thickness burns in many clinical guidelines [18]. SSD, synthesized by Charles Fox in the 1960s, remains the gold standard topical antimicrobial agent for burn treatment and approval was received from the U.S. Food and Drug Administration (FDA) [19]. It exhibits broad-spectrum antimicrobial efficacy against a wide range of pathogenic microorganisms such as P. aeruginosa and S. aureus [20]. Its primary mechanism of action involves the gradual release of silver ions, which bind with bacterial DNA by binding to the helical structure and inhibiting transcription processes [21]. Traditional SSD cream formulations present several significant limitations, such as limited skin penetration, toxicity resulting from rapid silver ion release, discomfort during reapplication, and an elevated risk of bacterial resistance with prolonged use [20].

In contrast, nano-enabled approaches have demonstrated considerable promise in addressing and potentially overcoming these challenges. Nanotechnology has shown significant potential to enhance wound healing through targeted delivery of antimicrobials and therapeutically active compounds. Nanomaterials such as nanoparticles, nanofibers, nanogels, and nanoemulsions improve drug stability, skin permeation while providing sustained drug release at the site of injury. Over the past decade, nanotechnology-enabled drug delivery platforms have attracted considerable research interest for improving topical burn therapies. Nanocarriers such as liposomes, ethosomes, niosomes, cubosomes, and polymeric nanoparticles enhance drug stability, penetration, and controlled release profiles. These systems facilitate targeted delivery, reduce dosing frequency, and minimize systemic

toxicity. Among them, Transfersomes (TFs) offer a promising approach due to their ability to deliver drugs across the skin barrier efficiently. It exhibits ultra-flexibility, enabling it to reach deeper skin layers without structural compromise [22].

Originally, the term "transfersome" is traces back to Latin "transferre," that translates to "to carry across," and the Greek "soma," meaning "body". TFs are vesicular systems composed of phospholipids such as phosphatidylcholine and distearyl phosphatidylcholine, combined with edge activators (EAs), including sodium cholate, Tween 80, and Span 80. These EAs partially destabiliz the phospholipid bilayer, thereby enhancing its deformability and flexibility and thereby improving elasticity and skin penetration [23]. These highly deformable vesicles can pass through pores as small as one-tenth of their diameter, enabling drug-loaded vesicles to penetrate deeply into the dermal layers while maintaining structural integrity. Their unique architecture allows the encapsulation of both hydrophilic and hydrophobic drugs. Owing to their low viscosity, TFs can be conveniently incorporated into gel formulations, thereby enhancing skin retention and optimizing therapeutic efficacy. TFs gels provide additional benefits, few of them are such as release of gel in a well-controlled and sustained, enhanced patient adherence through decreased dosing rate, and enhanced tolerability, particularly for sensitive or compromised skin [24].

TFs gels represent an advanced approach in topical and transdermal drug delivery systems, adding the superior deformability of TFs with the desirable rheological and application properties of polymeric gels. TFs are radical flexible lipid vesicles composed of phospholipids and edge activators, enabling them to penetrate through the stratum corneum by squeezing through intercellular pathways, thereby enhancing drug permeation and bioavailability. However, due to their colloidal and liquid nature, transfersomal dispersions are commonly incorporated into gel matrices to improve stability, viscosity, and patient compliance. Among various gelling agents, Carbopol-based gels are widely used for their high viscosity, excellent bioadhesion, and controlled drug-release characteristics. A study by Batool et al. (2021) reported that Carbopol-based transfersomal gel of miltefosine

significantly enhanced skin permeation and targeted drug delivery for cutaneous leishmaniasis, demonstrating improved therapeutic efficacy compared to conventional formulations [25]. Beyond Carbopol, other polymers such as hydroxypropyl methylcellulose (HPMC), poloxamers, and alginates are also widely explored in transfersomal gel formulations due to their ability to modulate viscosity, drug release kinetics, and skin compatibility. Recent studies, such as the formulation of famciclovir-loaded transfersomal gel (2024), emphasize the importance of selecting appropriate gel matrices to enhance drug localization, permeation, and therapeutic outcomes [26].

Although SSD continues to serve as a cornerstone in burn management, its therapeutic performance could also be substantially enhanced by integrating it into a chitosan natured TFs gel system. Chitosan (Chi) is a naturally derived biopolymer known for its wide range of therapeutic properties, including antibacterial, antifungal, wound-healing, and immunomodulatory activities, and has pulled considerable focus due to its biodegradability, biocompatibility, and intrinsic permeation-enhancing traits. Chi carries a positive charge that facilitates electrostatic interaction with negatively charged skin components, thereby enhancing drug retention and penetration. Its antimicrobial efficacy has been shown to increase with higher degrees of deacetylation and greater molecular weight, underscoring its versatility and bioactive potential. Due to its broad-spectrum antimicrobial activity and diverse mechanisms of action, chi is highly promising for a range of biomedical and pharmaceutical applications.

Moreover, its capacity to stimulate inflammatory cell activity enhances tissue repair processes, supporting its role as an effective wound healing promoter and further emphasizing its clinical significance in therapeutic formulations [27]. This TFs-loaded gel combination enables deeper skin penetration, minimizes toxicity, and ensures localized, sustained antimicrobial activity at the site of infection.

The research relies on the development of SSD-loaded TFs as an innovative strategy to overcome the limitations of conventional SSD cream formulations. The primary objective is to enhance the therapeutic efficacy of SSD by improving its

infiltration into deeper skin layers, providing controlled and extended release of drug while minimizing the frequency of drug administration. This novel approach aims to increase the antimicrobial effectiveness of SSD while minimizing toxicity and improving patient compliance.

By employing a TFs delivery system, the study seeks to address the inherent drawbacks of traditional topical formulations, ensure localized and prolonged therapeutic action at the infection site, and ultimately provide a a more efficient and patient-compliant therapeutic approach for the management of bacterial infections associated with wounds.

1.2 Study Gap

SSD is a common topical antimicrobial for treating burn wounds, but traditional formulations have drawbacks such as poor skin penetration and frequent application requirements.

SSD incorporated TFs offer superior skin penetration, particularly when used in combination with chi to enhance antimicrobial and wound-healing effects, but this has not been sufficiently explored.

1.3 Problem Statement

Burn wounds are highly susceptible to infection due to the skin barrier disruption, which delays wound healing. Conventional dosage of SSD exhibited poor skin penetration, reduced retention time, reduced therapeutic efficacy, and thus requires frequent application [28].

Therefore, it is utmost urgency to develop an advanced delivery system that enhances skin penetration, provides sustained release, reduces the need for frequent dosing, and ultimately improves patient compliance and reduces wound infection.

1.4 Aim

To develop and characterize SSD-loaded TFs chi gel (SSD-TFs-Chi gel) for enhanced skin penetration, sustained SSD release, reduced dosing frequency, and improved antibacterial efficacy against skin wound infections.

1.5 Objectives

i. To prepare and optimize the SSD-TFs by the thin film hydration method.

ii. To evaluate and characterize SSD-TFs for *in vitro* characterization, including particle size, polydispersity index (PDI), zeta potential, morphology, entrapment efficiency, drug loading, Transmission Electron Microscopy (TEM), Attenuated Total Reflectance-Fourier Transform Infrared Spectroscopy (ATR-FTIR), and X-Ray Powdered Diffraction.

iii. To assess the release profiles of *in vitro* drug at pH 5.5 and 7.4, and explore the mathematical kinetics of the drug release from SSD-TFs.

iv. To incorporate SSD-TFs into a chi gel base to form SSD-TFs-Chi gel and investigate its physicochemical attributes, containing physical appearance, pH, viscosity, and spreadability.

v. Determination of SSD-TFs-Chi gel antibacterial efficacy against common wound pathogen (S. aureus), and assessment of *ex vivo* skin permeation and in *vivo* skin biocompatibility studies.

Chapter 2

Literature Review

2.1 Wound Infections

Wound infection is a major clinical problem that significantly impairs the normal healing process and can lead to chronic wounds, prolonged inflammation, and increased healthcare burden [29, 30].

The transition from contamination to infection is influenced by bacterial virulence, host immunity, and biofilm formation, which shields microbes from immune clearance and antibiotics [31].

De Francesco et al. (2022) reported that bacterial colonization significantly prolongs the inflammatory phase, making managing infection a critical step in wound care, and SSD reduced bacterial colonies and improved healing outcomes in chronic wound patients [32].

2.2 SSD: Physicochemical Properties

SSD is a sulphonamide-based antimicrobial widely used as widely used as a topical therapy for burn wounds owing to its ability to inhibit a broad range of both Gram-positive and Gram-negative bacterial pathogens [32]. SSD combines silver

ions with a sulphonamide moiety, enabling antibacterial action by interacting with bacterial DNA and enzymes. Its physicochemical limitations include poor solubility and poor penetration, which can reduce drug retention at the site of infection and require frequent reapplication. The hydrophobic nature of SSD also contributes to its slow diffusion through tissue barriers, hindering rapid penetration into deeper wound layers [33].

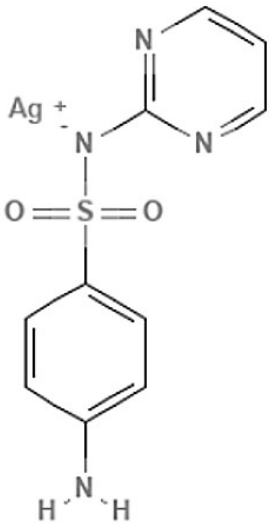

FIGURE 2.1: Chemical Structure of SSD

2.3 Conventional SSD Designs and Their Challenges

Traditionally, SSD has been formulated in creams and ointments for topical application in burn wounds [32]. Zhou et al. (2023) demonstrated a thermosensitive hydrogel containing SSD and chi that improved antibacterial effects and wound healing over conventional creams, highlighting limitations of standard formulations regarding sustained release and efficacy [34]. Pandey et al. (2020) developed breathable hydrogel sponges loaded with SSD, which showed better in vitro antimicrobial activity and faster wound closure compared to marketed SSD cream, addressing the challenges of poor SSD retention in conventional formulations [28]. Challenges with conventional SSD systems include:

i. Short drug retention and rapid wash-off.

ii. Poor penetration into deeper tissue layers [28].

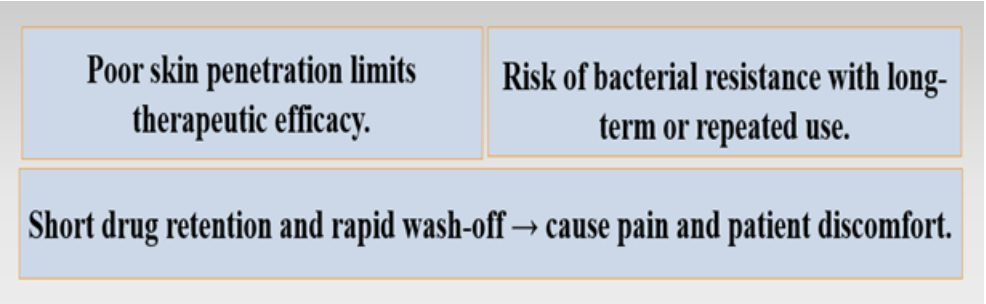

FIGURE 2.2: Limitations of Conventional Dosage Form

2.4 Advanced Drug Delivery Systems for Wound Healing

Recent research has focused on nanocarriers and advanced systems to overcome limitations of traditional formulations. Lopez Vidal et al. (2024) reviewed diverse advanced drug delivery platforms, including nanoparticles, nanogels, and wound dressings, to improve local therapeutic outcomes, enhance penetration, and sustain drug release [35]. Wang et al. (2019) summarized nano drug delivery systems, noting that functional nanosystems like polymeric nanoparticles and lipid carriers accelerate wound healing by sustaining drug release and enhancing therapeutic efficacy. These advanced systems address major barriers such as the stratum corneum penetration, localized drug delivery with minimal systemic exposure, and improved bioavailability at infection sites [36].

2.5 TFs and TFs Gels

TFs are ultra-deformable vesicular carriers designed to overcome skin barriers and improve skin penetration of therapeutic agents. Matharoo et al. (2024) describe TFs as flexible nanovesicles that can squeeze through tight skin intercellular spaces

and deliver drugs deeply, offering higher entrapment, release of sustained one, and importantly skin permeation improved compared to traditional systems [37].

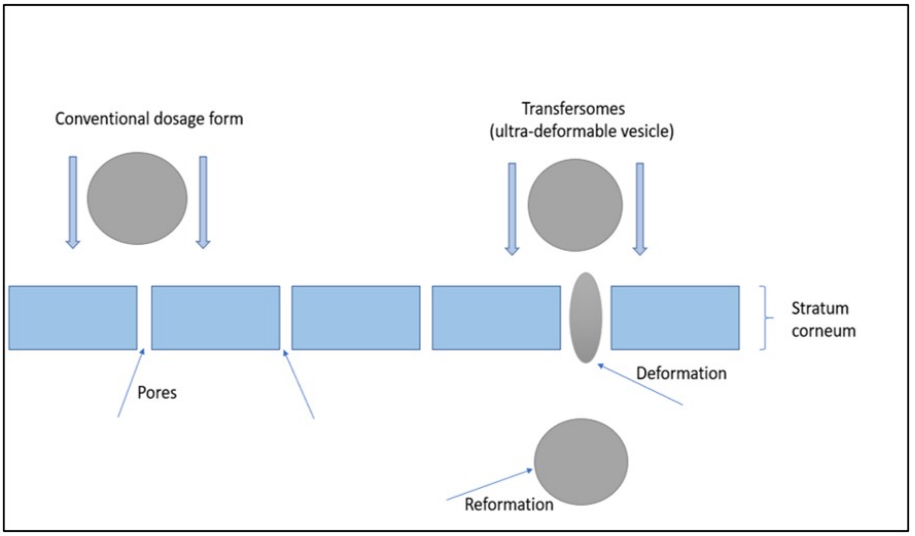

FIGURE 2.3: Systematic diagram of TFs vs conventional vesicles

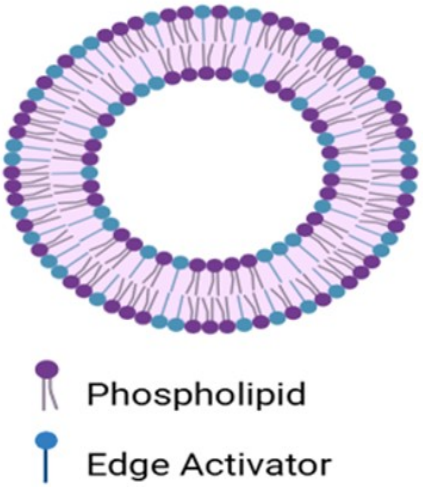

FIGURE 2.4: Composition of TFs

2.6 Methods for the preparation of TFs

TFs are prepared using several established techniques, among the commonly used available preparation techniques, thin-film hydration is the one of known employed approach. In this procedure, phospholipids and edge activators are first dissolved

in a volatile organic solvent system. The solvents are subsequently removed under reduced pressure to generate a uniform lipid film, which is later hydrated with an appropriate aqueous buffer, resulting in the spontaneous formation of vesicular carriers. The modified hand-shaking method involves solvent evaporation with continuous shaking above the lipid transition temperature, followed by hydration. In the vortexing sonication method, lipids and the drug are mixed in an aqueous medium, vortexed, and sonicated to obtain uniform vesicles. The ethanol injection method relies on the gradual addition of an ethanolic lipid solution into an aqueous phase, resulting in spontaneous vesicle formation. Vesicle characteristics can be further improved using the freeze–thaw method, which enhances lamellarity, or the reverse-phase evaporation method, where lipid emulsions are converted into vesicular suspensions by solvent removal. These methods enable efficient TFs formation with controlled size and drug encapsulation for transdermal delivery [38]. The thin-film hydration method is the most widely used and reliably produces nanosized, high-entrapment, deformable vesicles with good formulation flexibility.As compared with other methods, it offers a simple, reproducible, and effective composition, making it suitable for optimization for transfersomal formulations [21].

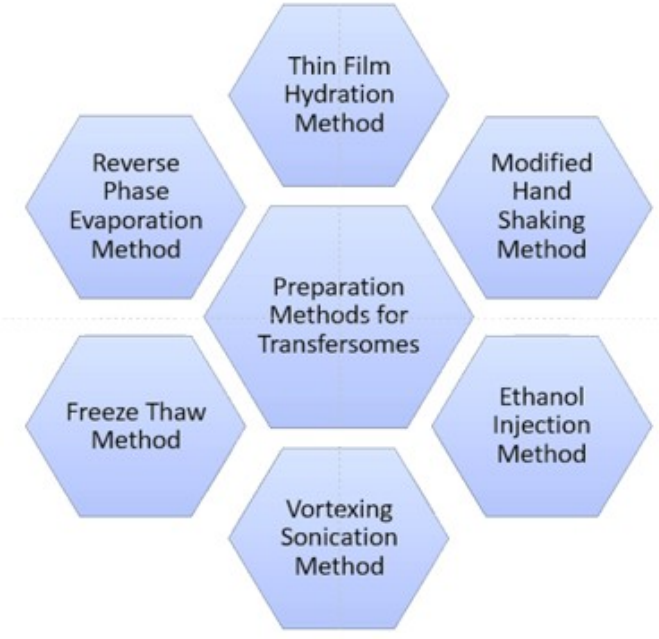

FIGURE 2.5: Methods for the Preparation of TFs

TABLE 2.1: Overview of SSD -Based Drug Delivery System

Authors	year	Lipid/Polymer Carrier	Formulation Type	Objective	Key Findings	Ref
Nascimento et al.	2025	Laponite hydrogel	Smart Hydrogel	Sustained Topical Delivery	Controlled Release, enhanced antimicrobial and antibiofilm activity	[39]
Mutlu-Agardan et al.	2022	Chitosan / PVP	Nanoparticle -loaded Nanofiber	Controlled release & antibacterial dressing	Sustained release against	[40]
Luo et al.	2020	Cyclodextrin metal-organic framework	Nano co-delivery system	Enhanced antibacterial function	∼50× increased SD solubility; stabilized nano-silver; improved antibacterial efficacy	[41]
Liu et al.	2017	Poloxamer 407	Nanosuspension thermosensitive Hydrogel	Enhance solubility & topical action	∼96.7% dissolution improvement; decreased cytotoxicity; enhanced antimicrobial effect	[42]
Al-Janabi & Al-Edresi	2025	Zein/PCL	Nanofibers	Improve release behaviour	Uniform nanofiber carrier; improved SSD release for topical use	[43]

Table 2.1 continued from previous page

Authors	year	Lipid/Polymer Carrier	Formulation Type	Objective	Key Findings	Ref
Barkat et al.	2017	Nanosuspension in Aloe vera gel	Nanosuspension gel	Improved wound healing activity	Significantly higher release & in vivo wound healing as compared to the marketed formulation	[44]
Razavi et al.	2018	Lipid-based system	Nanocarrier system	Burn treatment delivery	Comprehensive overview of lipid nanocarriers for SSD; improved therapeutic delivery potential	[45]
Razavi et al.	2018	Ethosomal vesicles	Nanoethogel	Enhanced burn healing	High encapsulation; enhanced wound healing	[19]
Venkataraman & Nagarsenker	2012	Nanosuspension or nanogel	Nanosuspension-based gel	Increased bactericidal activity & wound therapy	Nanosuspension-enhanced SSD wound healing vs commercial cream	[46]
El-Feky et al.	2017	Chitosan Nanoparticles	Nanoparticle-coated dressing	Controlled release in wound dressing	CSNPs loaded with SSD; improved controlled release potential for wound therapy	[47]

Table 2.1 continued from previous page

Authors	year	Lipid/Polymer Carrier	Formulation Type	Objective	Key Findings	Ref
Zhou et al.	2023	Chitosan hydrogel	Thermosensitive hydrogel	Promote wound healing	Sustained SSD release; enhanced antibacterial effect &wound healing in rat model healing in rat model	[34]
Vinayak Shivamurthi Mastiholimath et al.	2020	Solid lipids	Solid Lipid Nanoparticles	Develop a controlled-release topical delivery system for burn wounds	SLNs showed sustained drug release, enhanced stability, and improved therapeutic potential for second-third burns	[48]
Keisuke Ito et al.	2015	Inorganic nanosheets	SSD-loaded nanosheets	Enhanced antimicrobial efficacy in burn infection	Sustained antimicrobial activity and significant reduction of infection	[49]

Table 2.1 continued from previous page

Authors	year	Lipid/Polymer Carrier	Formulation Type	Objective	Key Findings	Ref
Waqas et al.	2022	Sodium alginate /polyvinyl alcohol	Electrospun Nanofibers	To fabricate SSD-loaded nanofibers for the prevention of burn wound infections	showed strong antibacterial activity against Staphylococcus aureus	[50]
Morsi et al.	2013	Poloxamer 407, Chitosan/Carbopol	Cubosomes-based Hydrogel	To develop cubosome hydrogels of SSD for topical burn treatment	Cubogels exhibited sustained drug release, improved bioadhesion, and enhanced healing of burns as compared to the marketed SSD.	[51]

TABLE 2.2: Overview of Chitosan-based Drug Delivery System

Authors	Year	Lipid/Polymer Carrier	Formulation Type	Objective	Key Findings	Ref
Khaqan et al.	2018	Chitosan	Thermosensitive Hydrogel	Sustained ophthalmic drug delivery	Developed an injectable thermosensitive gel showing controlled release.	[52]
Rinaudo et al.	2020	Chitosan	Hydrogel matrix	Sustained drug release	Demonstrated controlled drug release	[53]
Sabouri et al.	2026	Chitosan Nanogel	Dermal/transdermal nanogel system	Improved Dermal drug delivery	Demonstrated enhanced skin permeation, stability, and controlled release.	[54]
Zhang et al.	2024	Chitosan	Smart hydrogel	Controlled drug delivery system	Showed 3D porous network with sustained drug release.	[55]
Kazim et al.	2021	Glutaraldehyde + Chitosan with SLNs (Compritol, Tween 80)	Nanoparticle-loaded chitosan Hydrogel	Develop a topical system for allergic contact dermatitis using ebastine-loaded SLNs	Formulated hydrogel showed sustained drug release, improved stability and enhanced therapeutic efficacy.	[56]

2.7 Role of Chitosan in Wound Infection

Chi has emerged as a multifunctional polymer with inherent antimicrobial and wound-healing properties. Zhang et al. (2026) conducted a bibliometric analysis showing a growing global research focus on chitosan-based infected wound care, confirming chitosan's increasing application in antimicrobial wound dressings [57].

Alven & Aderibigbe (2024) reviewed chitosan-based scaffolds with silver nanoparticles that enhanced antimicrobial activity and accelerated re-epithelialization in infected wounds, showing synergistic antimicrobial and wound-healing effects [58].

Barkat et al. (2025) developed an SSD-loaded nanosuspension incorporated into a chitosan nanogel, which improved SSD solubility, sustained release, spreadability, and skin tolerability, ultimately yielding superior wound healing compared to conventional SSD products [33].

Chi has also been investigated to boost the antimicrobial nature of SSD formulations by improving moisture retention, sustained release, and biocompatibility [28].

Chapter 3

Materials and Methods

3.1 Materials

USP grade SSD was obtained from Davis Pharmaceutical Industry, Islamabad, Pakistan. Lipid component Soya Lecithin, along with surfactant Tween 80, was bought directly through Sigma Aldrich (CHEMEI GmbH, Germany). Methanol was obtained from Duksan Chemicals, Korea. Chloroform and Chitosan were also procured directly through Sigma Aldrich (CHEMEI GmbH, Germany). Distilled water and Phosphate Buffer Solution (PBS) were freshly prepared at the Faculty of Pharmacy, Capital University of Science and Technology (CUST), Islamabad.

3.2 Method

3.2.1 Preparation of SSD-TFs

SSD-TFs were formulated using the thin-film hydration technique [59]. Briefly, a chloroform: methanol (1:1) solvent system was used to dissolve SSD, soy lecithin, and Tween 80. To create a thin lipid film, the organic solvents were evaporated by a rotary vacuum evaporator at 45 ± 1 °C under lower pressure. After that, resulting lipid film was rehydrated using phosphate-buffered saline (PBS) and

rotated at 45 ± 1 °C to allow the lipid vesicles to swell fully. The suspension was sonicated to obtain uniformly sized TFs [59].

TABLE 3.1: Composition of Formulations

Formulation codes	**Phospholipid amount (mg)**	**Surfactant amount**	**Volume of hydration medium**	**Amount of drug**
		(mg)	**(ml)**	**(mg)**
F 1	40	10	5	2
F 2	30	10	5	2
F 3	20	10	5	2
F 4	40	20	5	2

3.2.2 Preparation of SSD-TFs gel

The optimized TFs dispersion was gradually added to a chi gel (200 mg of chitosan powder was weighed and then mixed in 5 milli Liter (mL) of 1 percent v/v acetic acid) with constant agitating for 5 minutes to prepare the SSD-TFs gel [56].

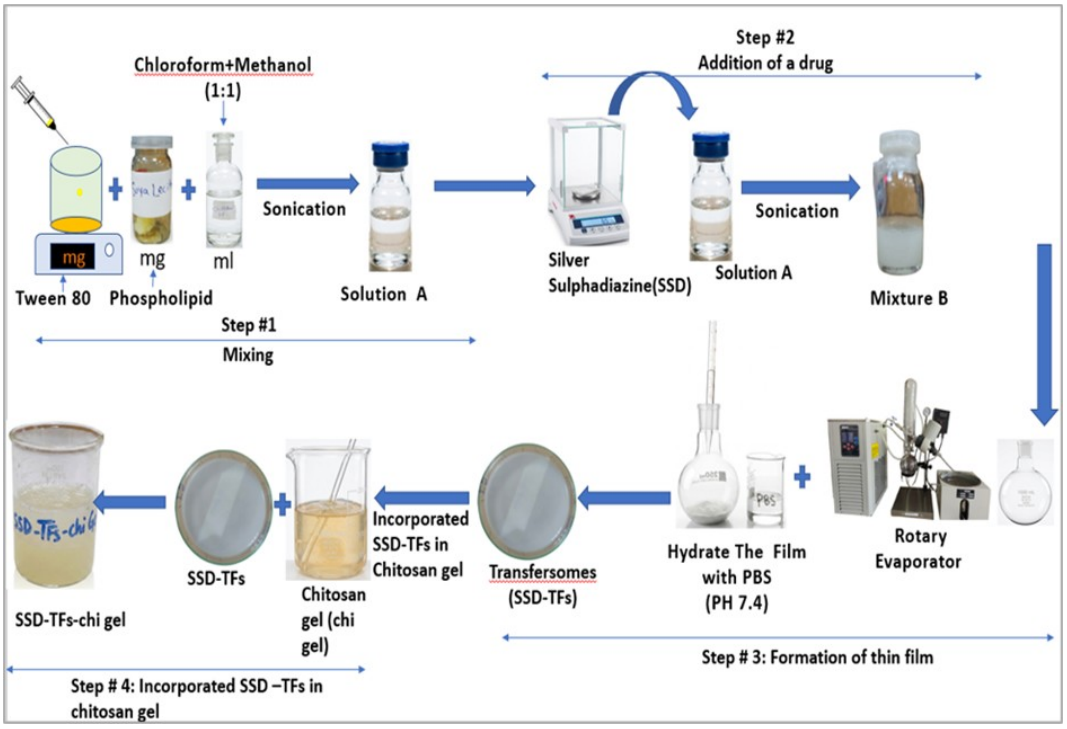

FIGURE 3.1: Method of Preparation of TFs

3.2.3 Lyophilization of SSD-TFs

Before freeze drying, the formulation was placed at -20 °C for 8 hours to ensure complete freezing.

Lyophilization was subsequently carried out in two sequential stages: primary drying at -40 °C for 12 hours, pursued by secondary drying at 25 °C for an additional 12 hours.

FIGURE 3.2: Lyophilizer

3.3 *In vitro* Characterization

3.3.1 Particle Size, Polydispersity Index and Zeta Potential

The particle size and polydispersity index (PDI) of SSD-TFs were calculated with a Zetasizer Nano ZS90 from Malvern Instruments (UK). The collected samples were kept at 25 ± 2 °C. We performed laser light scattering analysis using a laser beam at a scattering angle of 90°. We also measured the surface charge (zeta potential) of SSD-TF vesicles with the same instrument [60].

3.3.2 Entrapment Efficiency and Drug Loading

The entrapment efficiency of SSD-TFs was measured using an indirect method. The prepared SSD-TFs were centrifuged at 13,500 rotation per minute for 30 minutes to separate the non-encapsulated drug fraction.

We quantified the amount of free SSD in the supernatant with UV-Vis spectrophotometry at λmax 254 nm. EE% and DL were determined by looking into the below equation [59].

$$\text{EE}(\%) = \frac{\text{Total drug content} - \text{Free drug content}}{\text{Total drug content}} \times 100 \tag{3.1}$$

$$\text{DL} = \frac{\text{Total drug content} - \text{Free drug content}}{\text{Total amount of transfersomes}} \tag{3.2}$$

3.3.3 *In Vitro* Drug Release

The release profile of *in vitro* drug was evaluated through the dialysis bag diffusion approach [56].The drug release from SSD-TFs and the drug was studied at pH 5.5 and 7.4. Formulations containing 2 mg of drug were individually dispersed in 5 mL of phosphate-buffered saline (PBS, pH 5.5 or 7.4) and transferred into dialysis bags. Each bag was subsequently placed in 50 mL of the respective PBS release medium and incubated in a shaking water bath maintained at 36 ± 2 °C with continuous agitation at 100 rpm for 48 hours.

At specified sampling times (0, 0.5, 2, 4, 6, 8, 10, 24, and 36 hours), collected samples from the release medium were instantly substituted with an equal volume of fresh buffer to preserve sink conditions. The cumulative release data were then evaluated using DD Solver by applying several mathematical models, namely zero-order, first-order, Higuchi, and Korsmeyer–Peppas, to determine the most appropriate kinetic model and gain insight into the mechanism governing the release of the drug [59].

3.3.4 Attenuated Total Reflectance-Fourier Transform Infrared Spectroscopy

The ATR-FTIR studies were performed to evaluate drug-excipient compatibility. The ATR-FTIR spectra of the pure components and selected SSD-TFs formulation were compared using an ATR-FTIR spectrophotometer (Bruker Alpha GmbH, Germany) at a wavenumber region of 4000-400 cm1.

Any interaction between SSD, Soya lecithin, Tween 80, and transfersomes was evaluated using this method [61].

3.3.5 X-ray Powder Diffraction

The crystalline or amorphous nature of the SSD-TFs and pure SSD was investigated using XPRD. The diffraction patterns of the compound were analyzed inside the formulation by an X-ray Diffractometer (Bruker D2 Phaser, USA). The samples were scanned using the standard operating conditions, scanning range of 10°–80° (2) [62].

3.3.6 Field Emission Transmission Electron Microscopy

FETEM was employed to characterize the morphology of the formulation, structural characteristics, and particle size distribution of the optimized SSD-TFs. A drop of the optimized transfersomal formulation was put on a carbon-coated copper grid for TEM characterization. After removing the excess dispersion with filter paper, the sample was negatively stained using 1% phosphotungstic acid. The stained grid was subsequently dried at ambient temperature and then visualized using a transmission electron microscope (Talos F200X G2, Electron Microscopy Centre, Fudan University China [59].

3.4 SSD-TFs-Chi Gel Characterization

The physical aspects, including appearance, homogeneity, and pH of the prepared SSD-TFs-chi gel, were analyzed to assess its potential for topical use.

3.4.1 Physical Appearance and pH

The formulated gel was assessed for colour, consistency, and phase separation. The pH of the formulation was figured out by dispersing 500 mg of chitosan TF gel in 20 mL of distilled water, followed by equilibration for 2 hours. After equilibration, the pH was recorded by a calibrated pH meter (PHS 25CW, BANTE Instruments, China) with the electrode inserted into the hydrated gel sample [56].

3.4.2 Spreadability

The spreadability of the SSD-TFs-chi gel was figured by the glass plate method. In short, 500 mg of the gel was deposited in the middle of a fixed glass plate (10 $\times$ 5 cm). A second glass plate of mass 5.75 $\pm$ 0.05 g was dropped from 5 cm from the height of the gel sample. Spread gel diameter was calculated after 60 second, and the spreadability was measured as a measure of the ease of application of the formulation to the skin [63].

3.4.3 Rheological Behaviour

The rheological properties of the SSD-TFs-loaded chitosan gel was analyzed by using a Brookfield DV2T viscometer (Spindle S 64) [56].

3.4.4 Antibacterial Activity

The antimicrobial potential of the formulated SSD-TFs-chitosan gel was assessed against Staphylococcus aureus by employing the agar well diffusion technique. A

bacterial suspension adjusted to the 0.5 McFarland standard was freshly prepared and uniformly distributed across Mueller–Hinton agar (MHA) plates using a sterile cotton swab to establish a confluent bacterial lawn.

The agar medium was added to wells with a diameter of about 6 mm using sterile cork borers. To ensure adequate diffusion of the semisolid gel formulation through the agar matrix, the SSD-TFs-chi gel and other test samples were dispersed in dimethyl sulfoxide (DMSO) before application. The concentration of DMSO was sustained below 10% (v/v) throughout the study to eliminate any potential antibacterial effect of the solvent [64].

The three experimental groups were SSD-TFs-chi gel, SSD-chi gel, and solvent control. 100 µL of individual sample was gently pipetted into individual wells. These inoculated plates were incubated for a period of 24 hours having temperature 37 ± 1°C under aerobic conditions. The antibacterial performance of each formulation was evaluated after incubation by determining the diameter of the clear growth inhibition zone around each well with a digital Vernier caliper.

The solvent control showed no inhibitory effect, indicating that the DMSO concentration used in the study did not interfere with bacterial growth. Each experiment was repeated three (3) times, and findings were showed as mean ± SD. One-way analysis of variance (ANOVA) was used for statistical analysis. For differences between groups, a p-value < 0.001 was considered statistically significant [64].

3.4.5 *Ex vivo* Permeation Study

Ex vivo permeation studies of SSD-TFs-chi gel were conducted on goat skin. Freshly excised goat skin was collected, and the hair was carefully shaved with an electric trimmer to maintain the integrity of the stratum corneum and ensure suitability for *ex vivo* permeation studies. Then, the skin was placed in warm water for easier trimming of fat and connective tissue that adhered to it. The skin was cleaned and then washed with PBS, blotted, wrapped, and stored at -30°C. It was equilibrated in PBS for about 30 minutes before experimentation.

The optimized SSD-TFs-chi gel and permeation characteristics of the SSD-chitosan gel were evaluated under *ex vivo* conditions using a Franz diffusion cell apparatus. Prior to the experiment, the excised skin was prepared and securely fixed between the donor and receptor compartments.

Phosphate buffer solution (PBS, pH 5.5) was used for the receptor compartment, ensuring complete contact with the lower surface of the skin and absence of air bubbles. A predetermined amount of SSD-TFs-chi gel and SSD-chi gel was respectively applied uniformly onto the skin surface within the donor compartment.

The experiment was performed at rotation of 500 rotations per minute with a temperature of 37 ± 0.5°C. The effective permeation area of the cell was 0.77 cm^2. The assembly was then firmly clamped together, preventing any leakage during the experiment.

During the permeation experiment, samples were periodically withdrawn from the receptor chamber and replenished with an identical volume of fresh PBS maintained at the experimental temperature, thereby ensuring sink conditions were maintained throughout the study.

The concentration of silver sulfadiazine in each collected aliquot was subsequently determined using a UV–Visible spectrophotometer by measuring absorbance at 254 nm.

The total quantity of drugs permeated/unit area was determined using the below equation:

$$Q_n = \frac{C_n V_r + \sum_{i=1}^{n-1} C_i V}{A} \tag{3.3}$$

Qn is the quantity of drug permeated per unit area ($\mu g/cm^2$) at the time of nth sample, Cn is the drug concentration in receptor fluid at the time of nth sample, Vr is the volume of receptor solution, $\sum C_i$ is the sum of the concentration of the drug in the receptor fluid before the nth sample, Vs is the Volume of the sample

withdrawn and A is the effective permeation area of the diffusion cell (0.77cm^2) [59].

3.4.6 Skin Irritation Study

The dermal biocompatibility and the irritation potential of the developed SSD-TFs-chi gel were assessed in healthy mice using the modified Draize skin irritation protocol [59]. The study was approved by the Research Ethics Committee of the Faculty of Pharmacy, Capital University of Science and Technology (CUST), Islamabad (CUST/DERC/PH/ERF/PG/2026/015), and experimental procedures were carried out as per the institutional guidelines for the care and use of laboratory animals.

Healthy mice were split into two experimental groups (n = 3 mice per group) for histopathological evaluation of skin irritation. Group I received the optimized SSD-TFs-chi gel and served as the test group to assess dermal compatibility. Group II was treated with 2% acetic acid solution, which served as the positive control to induce skin irritation and validate the sensitivity of the experimental model.

All mice were put under conditions defined by laboratory standard having (22 ± 2°C, 55 ± 5% RH, and 12 hours light/dark cycle) and had no restriction to standard pellet diet and water during the study. The abdomen skin surface of all mice divided in groups was carefully removed by shaving with an approved electric shaver, avoiding any cuts, abrasions, or damage to the skin surface, 24 hours before treatment. The area shaved was marked as a test area of about 4cm2. Each formulation was applied uniformly over the area with an appropriate amount by using a sterile spatula.

The treated skin surfaces were examined for erythema, edema, and irritation at 0, 2, 4, 8, and 18 h post-application. Severity of skin reaction was evaluated using the Draize scoring system: zero (0), no visible reaction; One (1), slight; two (2), moderate; 3, severe; 4, very severe. Irritation scores were obtained at

each observation time, and the dermatological tolerability of the preparations was assessed [59].

Following the 18 h observation period, the animals were sacrificed, and full-thickness skin samples were taken from the treated region for histopathological examination. The tissues thus collected were washed off gently with help of phosphate buffered saline (PBS) and then kept in 10% buffered formalin for 24 hours.

The sections of tissues placed on a clean glass slide and stained with hematoxylin and eosin (H&E). Histological examination was conducted under a light microscope to assess microscopic alterations, including epidermal integrity, inflammatory cell infiltration, dermal edema, vascular congestion, and preservation of skin appendages.

Histopathological changes were assessed through a modified semi-quantitative scoring framework. Each parameter was graded on a four-point ordinal scale ranging from 0 (normal) to 3 (severe alteration). The microscopic results of the treated groups were compared to the control groups to assess the dermal safety, biocompatibility, and irritation potential of the developed SSD-TFs-chi gel formulation [59, 65].

3.4.7 Stability Studies

The stability of optimized silver sulphadiazine loaded transfersomal chitosan gel (SSD-TFs-chi gel) was evaluated using the guidelines of ICH. The prepared formulation was maintained under various storage conditions, such as refrigerated (4 ± 2°C), room (25 ± 2°C), and accelerated (40 ± 2°C, 75 ± 5% relative humidity). The stability assessment was conducted at predefined time points (0, 1, 2, and 3 months). The formulation was visually inspected for any change in appearance, color, homogeneity, phase separation, and pH during each evaluation period. If no visible changes in the formulation occurred, like phase separation or colour change, and pH deviation did not exceed 0.5 units, that formulation seemed physically stable [66].

3.4.8 Statistical Analysis

All experimental data were elaborated as mean ± standard deviation (SD). Among groups, T-Test were performed to find the statistical comparisons. Each experiment was replicated three times (n = 3), and the outputs were expressed as means ± SD. The level of importance was 0.05*(a=0.05), 0.01**(a=0.01), and 0.001***(a=0.001).

Chapter 4

Results and Discussion

4.1 UV-Visible Calibration Curve

A calibration curve for SSD was created at a wavelength of 254 nm. This curve is essential for measuring drug concentration in solution using UV-Visible spectrophotometry and for ensuring precision in subsequent formulation studies. The calibration curve demonstrated a linear relationship between absorbance and concentration across the range of 2–12 µg/mL [48]. The calibration curve displayed a steady increase in absorbance with an increase in drug concentration, confirming compliance with Beer-Lambert's law within this range.

The regression equation from the calibration curve was:

$$y = 0.0048x - 0.0003 \tag{4.1}$$

where:

y = absorbance

x = concentration (µg/mL)

slope (m) = 0.0048

intercept (c) = -0.0003

TABLE 4.1: Concentration vs Absorbance

Calibration Curve at PH 5.5	
Concentration (µg/mL)	**Absorbance**
2	0.011
4	0.019
6	0.026
8	0.037
10	0.047
12	0.059

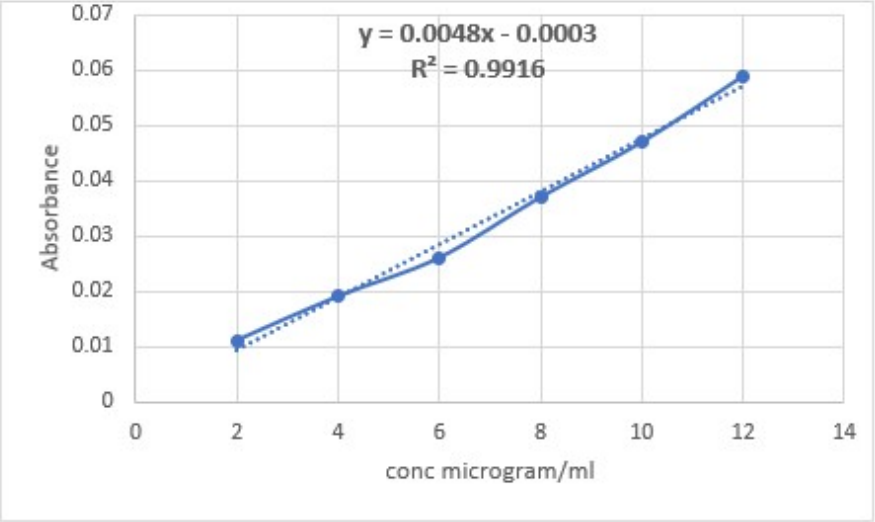

FIGURE 4.1: Calibration Curve

The slope shows the sensitivity of the analytical method, indicating a proportional increase in absorbance with concentration. The coefficient of determination (R^2 = 0.9916) reflects positive linearity and reliability of the protocol across chosen concentration range. This high R^2 value indicates minimal deviation of the experimental data from the regression line, affirmed that the protocol adopted is right for quantitative analysis of SSD.

4.2 Entrapment Efficiency

The percentage EE of formulations (F1–F5) was primarily influenced by the concentrations of phospholipid (soya lecithin) and Tween 80.

These two formulation variables were selected because phospholipids form the transfersomal bilayer responsible for drug encapsulation, whereas Tween 80 acts as an edge activator that imparts vesicle flexibility, enhances deformability, and significantly affects drug loading and vesicle stability [67], as represented in below Table 4.2 and subsequent Figure 4.2.

TABLE 4.2: Entrapment Efficiency (%) of transfersomes formulations

Formulation	**% EE**
F1	71.7 ± 2.79%
F2	85.5± 3.48%
F3	55.3 ± 3.02%
F4	54.8 ± 3.32 %
F5	48.6± 3.36%

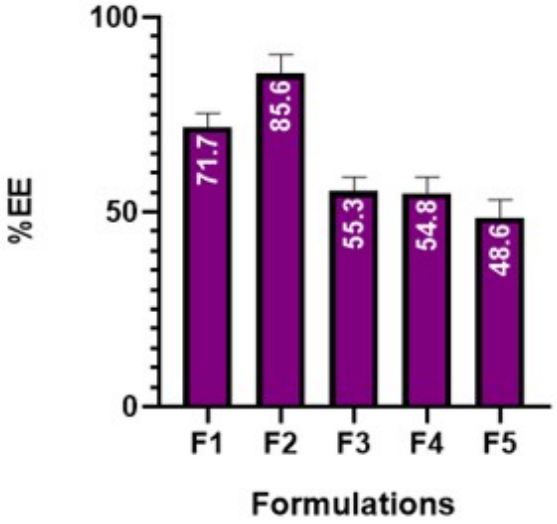

FIGURE 4.2: % Drug Entrapment Efficiency of Transfersomal Formulations

Formulation F1 contained 40 mg of phospholipid and 10 mg of surfactant, yielding a moderate %EE of 71.73 ± 2.79%. The formulation F2 showed %EE of 85.55 ± 3.48% when the phospholipid concentration was reduced to 30 mg, with the surfactant concentration held constant.

This suggests that an optimal level of phospholipids supports vesicle formation and improves drug encapsulation. However, reducing the phospholipid concentration further to 20 mg in formulation F3 led to a significant drop in %EE to 55.30 ± 3.02%. This decrease may be due to inadequate lipid matrix formation, which affects structural integrity and reduces the capacity to encapsulate the drug effectively.

On the other hand, formulations F4 and F5, which had surfactant concentrations increased to 20 mg and 30 mg, respectively, while keeping the phospholipid at 40 mg, showed a notable decline in %EE to 54.84 ± 3.32% and 48.63 ± 3.36%. The lower entrapment efficiency at higher surfactant levels might result from increased membrane fluidity, which can lead to drug leakage and reduced encapsulation.

The observed variation in entrapment efficiency among the formulations (48.6–85.5%) may be attributed to variations in phospholipid and Tween 80 concentrations. Phospholipids provide the bilayer matrix responsible for drug encapsulation, whereas an optimum concentration of Tween 80 enhances vesicle deformability and drug loading. However, excessive surfactant can disrupt the stability of the phospholipid bilayer, resulting in enhanced drug leakage and diminished entrapment efficiency.

Optimization of formulation is essential for developing efficient drug delivery systems with improved encapsulation performance. These findings are in agreement with previous reports, which demonstrated that the phospholipid-to-edge activator ratio is a critical determinant of transfersomal entrapment efficiency and vesicle stability [68].

The drug loading (DL) of the optimized SSD-TFs was observed to be 40 µg/mg, indicating efficient incorporation of SSD into the transfersomal vesicles.

4.3 Particle Size, Polydispersity Index, and Zeta Potential

The prepared SSD-TFs formulation gave a vesicle size (Z-average) of 148.0 nm, polydispersity index (PDI) of 0.179, and a zeta potential of 19.5 mV, as revealed in Figure 4.3. The vesicle size of the nanometric showed the successful preparation of the transfersomes and confirmed the suitability of the selected compositions (soya lecithin and tween 80) for the preparation of nanosized vesicular carriers.

The vesicles are relatively small, which is beneficial for topical drug delivery because it provides more surface area for the release of the drug and more contact between the vesicles and the skin. Nanosized transfersomes have been reported to penetrate the stratum corneum better than rigid liposomes because of their deformability, as well as the capacity to penetrate narrower intercellular pathways [69].

Tween 80 is a non-ionic surfactant that acts as an edge activator, decreasing the interfacial tension and increasing the flexibility of the phospholipid bilayer during vesicle formation, which may be responsible for the formation of small vesicles [70].

The PDI value of 0.179 indicated a narrow size distribution with uniform and homogenous vesicles and suggested a uniform incorporation of SSD. Generally, PDI values below 0.3 are typically regarded as good uniformity and reproducibility of the system and are considered to mark the presence of a monodisperse system.

The homogeneity is desirable to obtain consistent drug loading, predictable release behaviour, and improved physical stability during storage. The optimized formulation exhibited a moderately negative zeta potential of -19.5 mV, indicating that the vesicles had a surface charge of this magnitude. The negative charge can be due to the ionization of the phospholipid components of soya lecithin and the adsorption of surfactant molecules at the vesicle surface.

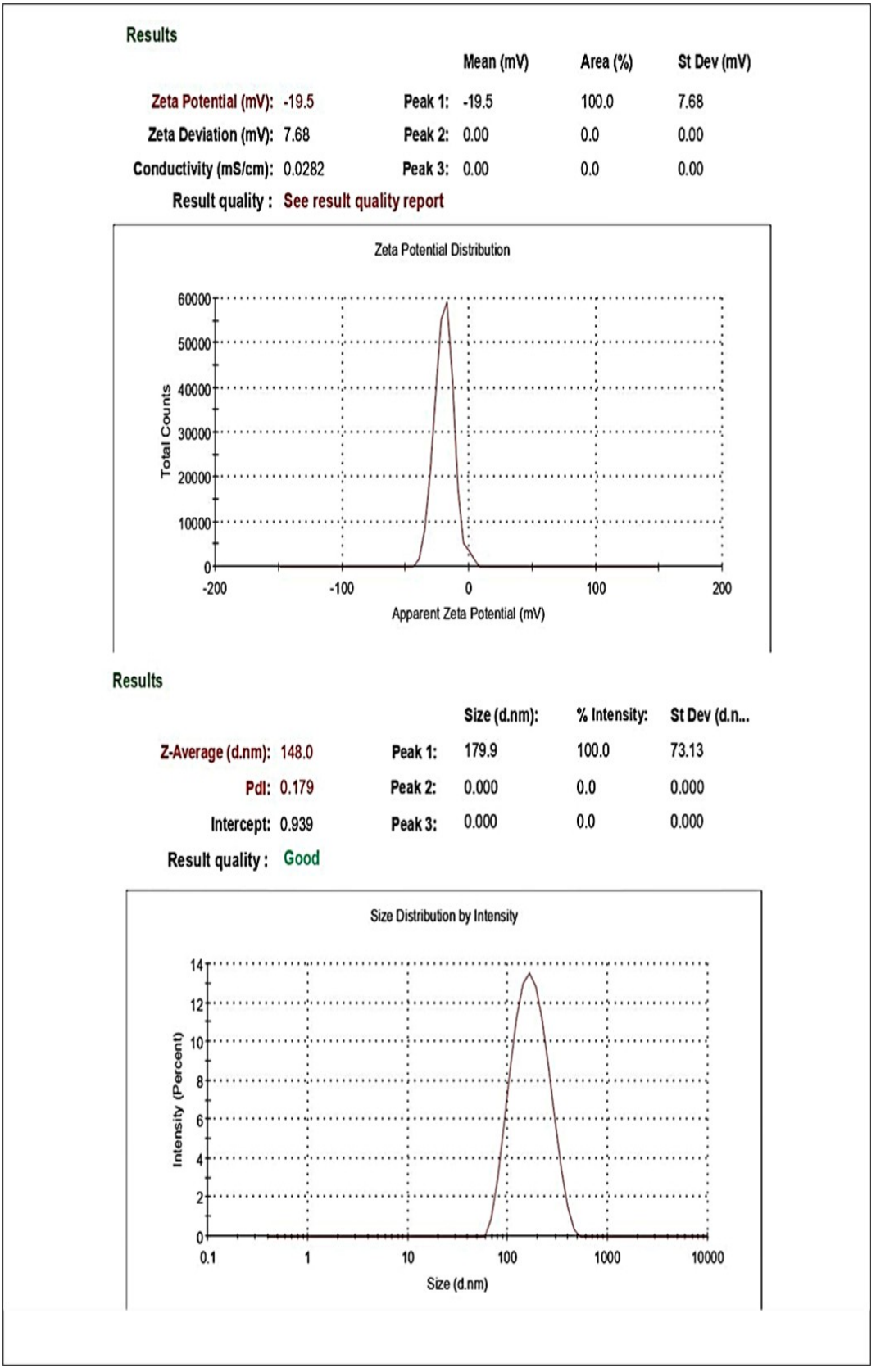

FIGURE 4.3: Zeta Potential, Z-Average, PDI of the optimized SSD-TFs confirming nanosized, colloidal stability and uniform distribution

TABLE 4.3: Physicochemical properties of optimized Formulation

Formulation	**Lipid (mg)**	**Surfactant (mg)**	**Drug**	**% EE**	**Zeta Potential (mv)**	**Particle Size (nm)**	**DL (μg/mg)**
F2	30	10	2	80.15	-19.5	148	40

The optimized formulation of SSD-TFs showed an appropriate vesicle size, low polydispersity index, and a moderately negative zeta potential, which indicated a successful development of a homogeneous nanosized vesicular system for topical delivery. The effect of the soya lecithin and Tween 80 resulted in stable and deformable vesicles, which could enhance the dermal delivery of SSD.

4.4 Attenuated Total Reflectance-Fourier Transform Infrared Spectroscopy

The ATR-FTIR spectra of soya lecithin, Tween 80, and optimized formulation containing SSD, as shown in Figure 4.4, were analyzed to examine the compatibility among the formulation ingredients and confirm the successful incorporation of the optimized formulation.

The ATR-FTIR spectrum of soya lecithin exhibited typical absorptions for its phospholipid composition. A broad absorption peak was seen in the range 3200–3400 cm^{-1} due to O–H stretching vibrations, which were linked to hydrogen bonding. The asymmetric and symmetric C–H stretching vibrations of aliphatic hydrocarbon chains occurred around 2920 cm^{-1} and 2850 cm^{-1}. Moreover, the strong band around 1730 cm^{-1} is assigned to the carbonyl (C=O) stretching vibrations characteristic of ester groups, which is characteristic of the phospholipid

structure of lecithin. The characteristic bands of the P=O stretching vibrations of phosphate ester groups in lecithin-based lipid systems appear in the ranges 1230–1240 cm^{-1} and 1090 cm^{-1} (Figure 4.4(a)), which corresponds to the literature [67].

ATR-FTIR spectrum of Tween 80 (Figure 4.4 (b)) showed the characteristic functional groups of a non-ionic surfactant. The O–H stretching broad peak at 3400cm^{-1} and the strong peaks around 2920 cm^{-1} were suggested to be aliphatic C–H stretching from long hydrocarbon chains. A special absorption band at 1730 cm^{-1} was experienced, which was assigned to the stretching vibrations of the carbonyl group of esters [71].

ATR-FTIR studies of pure SSD (Figure 4.4 (c)), showed a prominent absorption band at 3343 cm^{-1}, attributed to the stretching vibrations of the N–H group of the sulfonamide group.

The two aromatic ring/C=N stretching vibrations of the pyrimidine moiety were identified as a prominent peak at 1599 cm^{-1} and S=O stretching at 1016 cm^{-1}. The absorption bands are related to those previously reported in FTIR spectra of Silver Sulphadiazine, which led to its identification and the establishment of its structural integrity [16].

The ATR-FTIR spectrum of the formulated product with SSD, soya lecithin, and Tween 80 revealed the major characteristic peaks of all the formulation ingredients, with slight shifts and changes in intensity as shown in Figure 4.4 (d).

The wide absorption band at 3200–3400 cm^{-1} indicated the presence of intermolecular hydrogen bonding between the formulation components, probably due to the overlapping of the O–H and N–H stretching vibrations.

The characteristic peaks of aliphatic C-H stretching were seen around 2920 cm^{-1}, while the carbonyl stretching peak was also observed at the same position as that observed in the spectra of the lipids and surfactants before the formulation preparation, which indicates that the functional groups of lipids and surfactants are also retained after the formulation preparation. These results suggest that

there is no chemical incompatibility with the excipients used in the formulation and SSD.

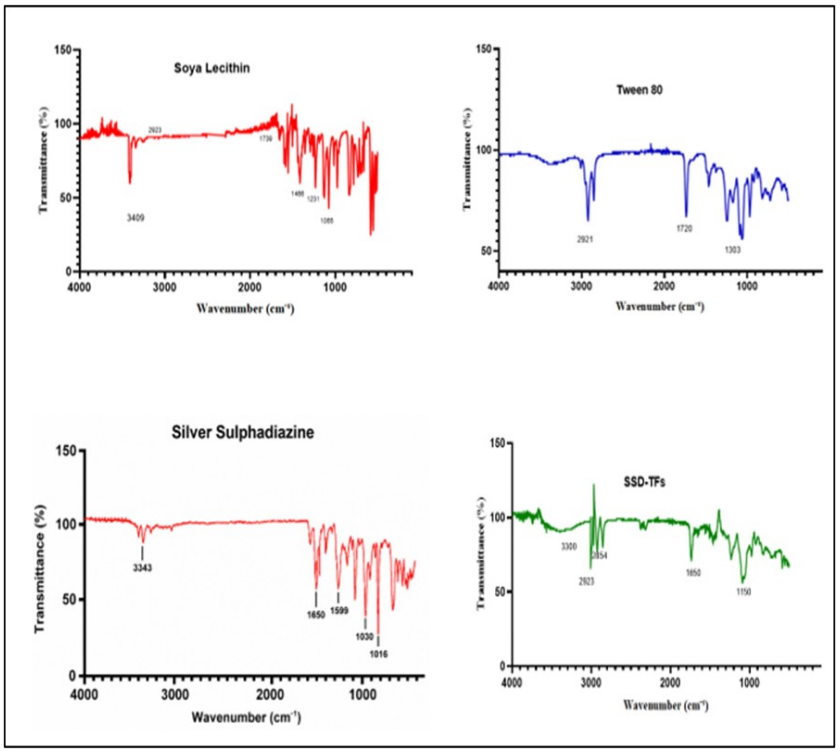

FIGURE 4.4: ATR-FTIR of (a) Soya Lecithin, (b) Tween 80, (c) Drug (Silver Sulphadiazine), (d) SSD-TFs (Silver Sulphadiazine Transfersomes)

4.5 X-Ray Powder Diffraction

XPRD was performed to assess the nature and potential structural modifications of SSD within the optimized SSD-TFs (Figure 4.5).

The XPRD pattern of pure SSD (Figure 4.5 (a)) showed intense and sharp diffraction peaks, indicating its highly crystalline nature. The most prominent peak was observed at 10°-12°, along with several additional sharp reflections between approximately 18° and 40°. The presence of these narrow and well-defined peaks indicates an ordered crystal lattice structure of SSD. These findings are consistent with previous reports showing the highly crystalline nature of silver sulphadiazine before encapsulation into lipid-based nanocarriers [62]. In contrast, the XRD pattern of SSD-TFs (Figure 4.5 (b)) showed a reduction in peak intensity and the

appearance of a broad diffuse halo, particularly around 18°–25°. This change suggests that SSD was successfully incorporated into the lipid vesicular system and converted from a crystalline form into a more amorphous or molecularly dispersed state. The broad halo observed in the formulation may be attributed to the lipidic nature of soya lecithin and the presence of Tween 80, which can disturb the regular structure of drug crystals and promote drug dispersion within the vesicular bilayer [62]. The disappearance and reduction of characteristic SSD peaks in SSD-TFs indicate that there was no separate crystalline drug phase in the optimized formulation. This finding supports the successful entrapment of SSD within the transfersomal carrier. Similar behavior has been reported for silver sulphadiazine nanosuspension and hydrogel-based systems, where XRD peak intensity was reduced after formulation, suggesting partial amorphization and weakening of the crystalline state of SSD [42].

The presence of soya lecithin and Tween 80 was also involved in the structural modification of the formulation. Tween 80 acts as an edge activator and increases vesicle flexibility, while Soya lecithin forms the phospholipid bilayer of TFs. Their combined effect may reduce the crystallinity of SSD by enhancing drug accommodation within the lipid matrix. Previous studies on lecithin-based deformable TFs have shown that Tween 80-containing vesicles can enhance drug release due to improved vesicular deformability [72]. The amorphous or molecularly dispersed state of SSD in SSD-TFs may contribute to better release performance and enhanced topical delivery potential compared with pure crystalline SSD.

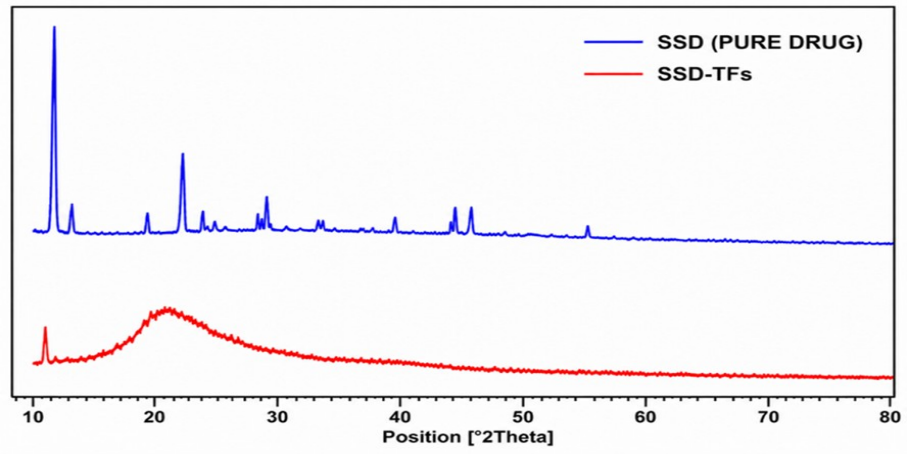

FIGURE 4.5: XPRD Diffractogram (a) Pure Silver Sulphadiazine (b) SSD-TFs

4.6 Field Emission Transmission Electron Microscopy

FE-TEM was carried out to analyze the morphology and structural properties of the SSD-TFs. The FE-TEM micrographs (Figure 4.6) illustrated the formation of nanosized vesicular systems, which appeared to have a distinct boundary and were mainly spherical to nearly spherical in shape. The majority of vesicles were seen to be discrete and structurally intact, suggesting good assembly of the phospholipid bilayer system using soya lecithin and the surfactant Tween 80. The vesicles in the micrographs, as indicated by the scale bars (100 - 200 nm), were characterized by comparatively smooth outlines and high contrast within. Some particles were found in a clustered pattern, which might be due to vesicle adhesion during drying and staining of the specimen on the grid.

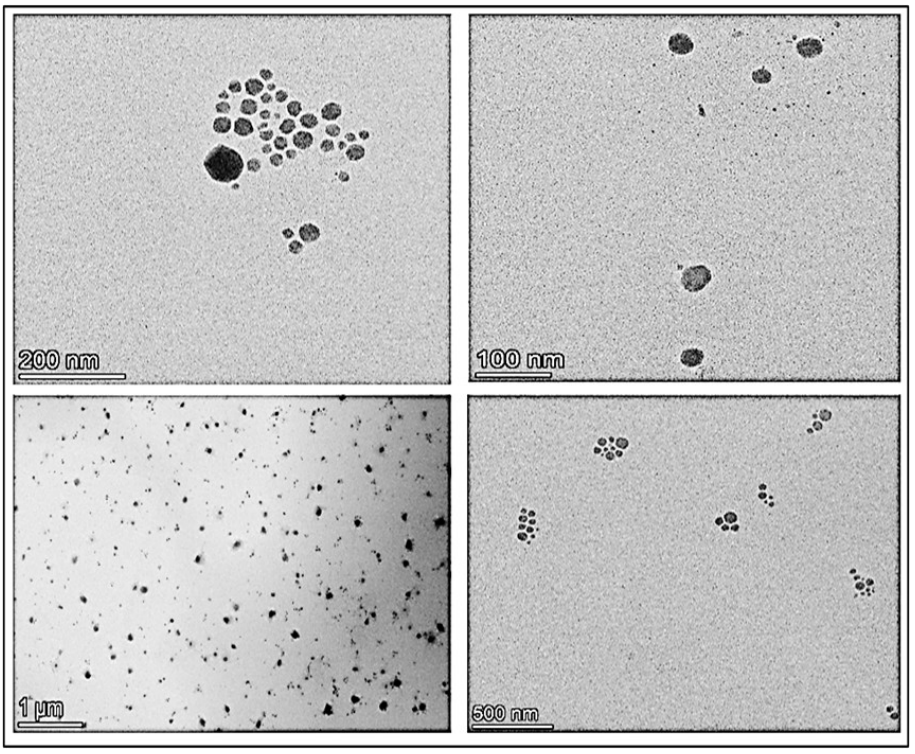

FIGURE 4.6: FE-TEM images of SSD-TFs

The spherical morphology observed in the formulation is consistent with the expected ultra-deformable structure of transfersomes, in which phospholipids self-assemble into closed bilayer vesicles, with Tween 80 serving as an edge activator

that makes the membrane flexible and reduces vesicle rigidity. The addition of Tween 80 probably helped to stabilize the vesicles because of its effect on reducing interfacial tension and enhancing the elasticity of the membrane, and therefore prevented vesicular fusion. Similar TEM observations in which the spherical nanosized and evenly distributed vesicles are transfersomal vesicles prepared with the surfactant Tween 80 in lecithin-based vesicles [37]. The results obtained in TEM confirmed the proper preparation of SSD-TFs with their morphology and their nanosized dimensions, and with appropriate dispersion behavior. These results further confirm the suitability of the developed formulation for topical application.

4.7 *In vitro* Drug Release

The *in vitro* release profile of SSD and the SSD-TFs was analyzed under two physiologically relevant conditions, pH 5.5 and pH 7.4. The cumulative percentage drug release profiles are shown in Figure 4.7 (pH 5.5) and Figure 4.8 (pH 7.4).

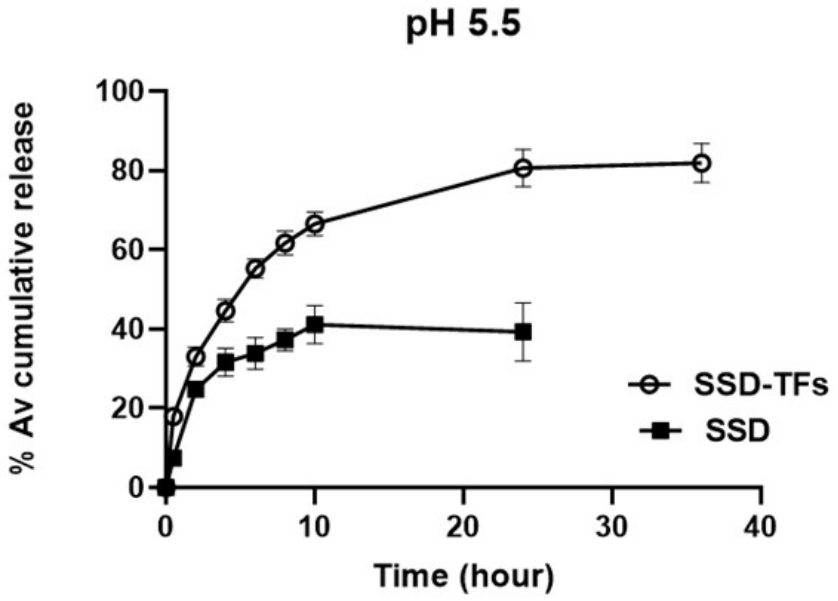

FIGURE 4.7: Cumulative Percentage release profile of SSD-TFs and the plain drug at pH 5.5. Values are expressed as mean ± SD(n=3)

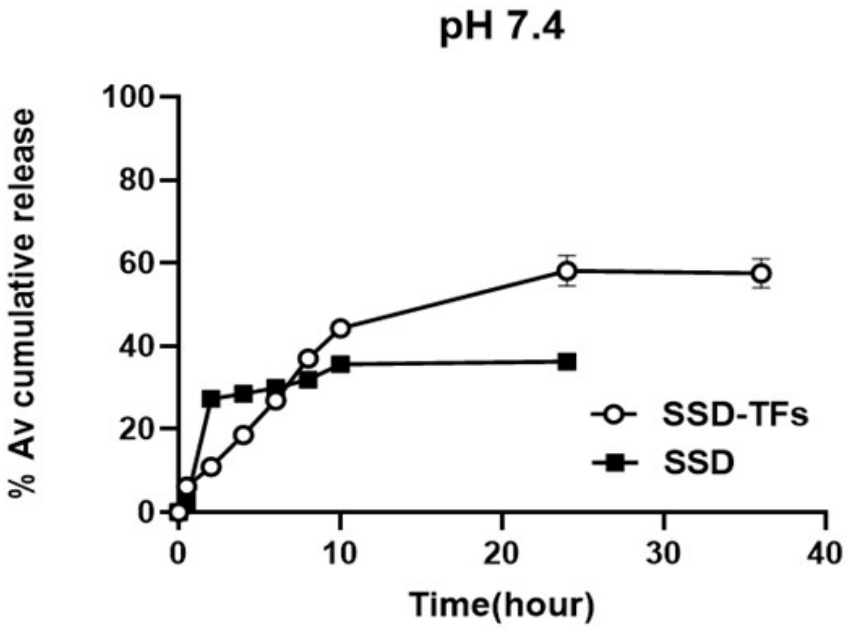

FIGURE 4.8: Cumulative Percentage release profile of SSD-TFs and the plain drug at pH 7.4. Values are expressed as mean ± SD(n=3)

At pH 5.5, conventional silver sulphadiazine (SSD) exhibited a relatively slow and incomplete drug release profile throughout the study period (Figure 4.7). An initial release of approximately 7% was observed within the first hour, which increased gradually to nearly 25% after 2 hours and reached approximately 41% at 10 hours. Thereafter, the release profile remained almost constant, indicating negligible further drug diffusion into the release medium. The moderate initial release can be attributed to the dissolution of SSD particles present at the surface of the formulation, whereas the subsequent plateau is mainly associated with the poor aqueous solubility and crystalline nature of SSD, which limit its dissolution and diffusion under mildly acidic conditions. Similar findings have been reported in recent studies, which describe conventional SSD as exhibiting limited aqueous solubility and low topical penetration, resulting in slow drug release and highlighting the need for advanced nanocarrier-based delivery systems to improve its release characteristics and therapeutic efficacy [33].

In contrast, the optimized SSD-TFs demonstrated a distinctly different release pattern. Drug release increased progressively without exhibiting a pronounced burst effect. Approximately 66% cumulative drug release was observed after 10

hours, which further increased to nearly 81% after 24 hours and remained almost constant until the end of the study. The sustained release profile indicates successful encapsulation of SSD within the phospholipid bilayer of the TFs , which gradually controls drug diffusion from the vesicular system. Moreover, the flexible nature of transfersomal vesicles and their large surface area facilitated continuous hydration of the lipid membrane, resulting in prolonged release of the encapsulated drug [62].

At pH 7.4, conventional SSD showed an immediate release during the early phase, attaining approximately 35% cumulative release within 10 hours as shown in Figure 4.8. Conversely, SSD-TFs displayed a controlled and sustained release profile, gradually increasing throughout the experimental period and achieving approximately 58% cumulative drug release after 24 hours. These findings demonstrate that transfersomal encapsulation significantly enhanced the release characteristics of SSD compared with the conventional drug under physiological conditions as shown in Figure 4.8.

The final cumulative release at pH 5.5 was approximately 81%, whereas only 58% was released at pH 7.4 during the same period. The increased release under acidic conditions may be attributed to alterations in phospholipid membrane fluidity, enhanced hydration of the vesicular bilayer, and greater drug solubilization at lower pH values. Such pH-responsive release behavior is particularly advantageous for topical wound therapy because infected wounds generally exhibit a slightly acidic microenvironment. Therefore, the formulation is capable of releasing higher concentrations of SSD directly at the site of infection while maintaining controlled release under normal physiological conditions.

Overall, the *in vitro* release study demonstrated that incorporation of SSD into TFs successfully overcame the limited release characteristics of the conventional drug by providing sustained drug release together with substantially higher cumulative drug release.

Drug release kinetic modeling demonstrated that the optimized SSD-TFs exhibited a predominantly diffusion-regulated release mechanism under both pH conditions.

TABLE 4.4: Kinetic Model fitting for SSD-TFs pH 7.4

pH 7.4 (SSD-TFS)					
	Zero order	First Order	Higuchi	Korsemeyer Peppas	Hixon Crowell
R	0.9079	0.9623	**0.9765**	**0.9768**	0.9468
R2	0.6449	0.8688	**0.9530**	**0.9465**	0.8071
AIC	66.6956	0.9530	**48.4865**	**50.4530**	61.2033
MSC	0.5646	1.5603	**2.5878**	**2.3693**	1.1749
MSE_root	12.8646	7.8194	**4.6780**	**4.9916**	9.4816
Others	k0=2.319	k1=0.040	**kH=11.244**	**kKP=11.542 n=0.491**	kHC=0.011

TABLE 4.5: Kinetic Model fitting for SSD-TFs at pH 5.5

pH 5.5 (SSD-TFS)					
	Zero order	First Order	Higuchi	Korsemeyer Peppas	Hixon Crowell
R	0.8277	0.9823	0.9555	**0.9880**	0.9770
R2	0.0199	0.8726	0.8491	**0.9722**	0.8140
AIC	80.4510	62.0861	63.6112	**49.1927**	65.4962
MSC	0.6909	1.3496	1.1802	**2.7822**	0.9707
MSE_root	27.6236	9.9582	10.8387	**4.6541**	12.0354
Others	k0=3.461	k1=0.124	kH=17.655	**kKP=29.679 n=0.312**	kHC=0.036

At pH 7.4, the Higuchi model demonstrated the optimal fit (R2 = 0.9530), indicating that drug release occurred primarily via diffusion from the phospholipid

matrix of the transfersomes, while the Korsmeyer-Peppas model (R2 = 0.9465, n = 0.491) subsequently confirmed a non-Fickian diffusion mechanism. In contrast, at pH 5.5, the Korsmeyer-Peppas model yielded the optimal fit (R2 = 0.9722) with a release exponent of n = 0.312, indicating Fickian diffusion as the primary release mechanism. Similar diffusion-controlled release behavior has been widely reported for phospholipid-based transfersomal systems, where the lipid bilayer acts as a diffusion barrier, providing sustained drug release and prolonged therapeutic action [69].

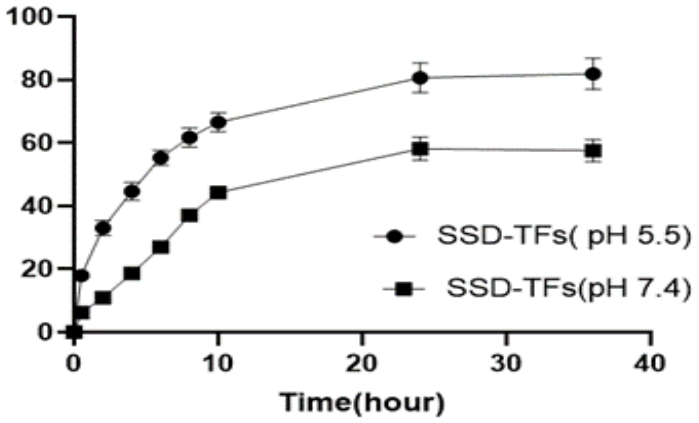

FIGURE 4.9: Cumulative Percentage release profile of SSD-TFs and the SSD-TFs. Values are expressed as mean ± SD(n=3)

4.8 Gel Characterization

4.8.1 Physical Appearance, pH, Viscosity, and Spreadability

The SSD-TFs-chi gel was evaluated for physical characterization, including pH, viscosity, and spreadability, to ensure suitability for topical application as shown in Table 4.6.

The developed SSD-TFs-chi gel exhibited a uniform appearance with a smooth consistency and remained free from visible signs of particle aggregation, grittiness, or phase separation. These observations indicate that the transferosomal

vesicles were successfully dispersed throughout the chitosan matrix, resulting in a physically stable gel system. The formulation showed a pH of 5.56 ± 0.03, which is compatible with the normal pH of healthy human skin (4.5–6.5), suggesting that topical application is unlikely to disturb the skin's natural acid mantle or cause irritation. Viscosity measurements revealed a value of 11,625 ± 329 cP, demonstrating that the gel possessed sufficient consistency to remain at the site of application while still allowing convenient handling during use. This rheological behavior is advantageous because it minimizes formulation runoff after application and enables uniform distribution over the skin surface. The measured spreadability of 4.42 ± 0.02 cm further confirmed that the gel could be evenly applied with minimal effort. The combination of suitable viscosity and satisfactory spreadability reflects a well-balanced gel structure, which is expected to improve patient acceptability while maximizing contact between the formulation and the affected skin area. [48].

The overall physical characterization results showed that the optimized SSD-TFs-chi gel has good properties for topical application. The formulation was found to possess the desired properties like pH, viscosity, and spreadability, which are the essential parameters to ensure patient comfort, retention at the site of application, and therapeutic efficiency.

TABLE 4.6: Physicochemical attributes and Rheological behavior of SSD-TFs Gel

Parameters	**Measured Value (Mean ±SD)**	**Observation**
Physical Appearance	Smooth texture, homogeneous	Homogeneous gel with no phase separation, which indicates a uniform distribution of particles.
pH	5.56±0.03	Falls within the physiological range of skin pH.

Table 4.6 continued from previous page

Parameters	**Measured Value (Mean ±SD)**	**Observation**
Viscosity (cp)	11625 ± 329	Provide adequate consistency for topical application.
Spreadability (cm)	4.42 ±0.2	Facilitate uniform application with no mechanical force.

4.8.2 Antibacterial Activity

The antibacterial activity of the developed SSD-TFs-chi gel was evaluated against S. aureus using the agar well diffusion method. After a 24 h incubation, the antibacterial activity of SSD-TFs-chi gel was evaluated and compared with that of the conventional SSD-chi gel and the blank chitosan gel, as shown in Figure 4.9.

The highest antibacterial activity was observed for SSD-TFs-chi gel, with a ZOI of about 28.5 mm at 24 h, whereas SSD-chi gel had a ZOI of 25.0 mm at 24 h. On the other hand, the blank chitosan gel exhibited a very small inhibition zone of about 7.5 mm.

Statistical analysis using one-way ANOVA demonstrated a significant difference among the formulations ($p = 0.02$), indicating the enhanced antibacterial performance of the TFs gel.

The enhanced inhibition zone observed with SSD-TFs-chi gel could be explained by the presence of SSD in nanosized TFs vesicles, which enhances the diffusion of the drug and prolongs the release at the site of infection [73].

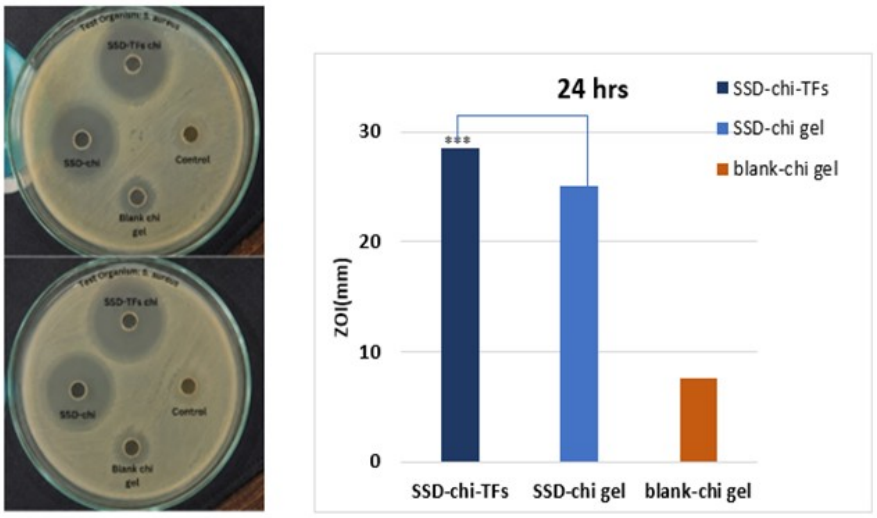

FIGURE 4.10: Antibacterial activity of SSD-TFs-chi gel, SSD-chi gel, Blank chitosan gel and Solvent against Staphylococcus aureus after 24 hr. Results are expressed as mean ±SD (n=3) and (*p <0.001)

Topically applied, SSD is effective against a wide range of Gram-positive is regarded as one of the most effective topical antimicrobial agents for application in wound management.

But traditional formulations of SSDs have poor penetration and drug availability at the target site. These drawbacks have been overcome using nano-based delivery systems, which have been reported to facilitate drug distribution, extend drug release, and improve the antimicrobial activity of the drugs [73].

The SSD-chi gel also showed considerable antibacterial activity owing to the presence of silver sulphadiazine, but the absence of a vesicular carrier system may have restricted drug diffusion through the agar medium.

However, the blank chitosan gel showed only trace amounts of antibacterial activity, suggesting that the activity might be due to the inherent antimicrobial properties of chitosan.

Therefore, the superior inhibition produced by SSD-TFs-chi gel demonstrated the potential of TFs carriers as an effective platform for topical application.

4.8.3 *Ex vivo* Permeation Studies

The *ex vivo* skin permeation study was performed to evaluate the ability of the optimized SSD-TFs-chi gel to enhance the transport of SSD across the skin compared with the SSD-chi gel. The experiment was performed using a Franz diffusion cell, and the cumulative amount of drug permeated through the skin was determined over 24 hours. The permeation parameters are presented in Table 4.7.

Table 4.7: Skin Permeation parameters of SSD-TFs-chi gel

Formulations	**Cumulative amount permeated for 24 hrs, Q24(µg/cm²)**	**Permeation flux, J(µg/cm²/h)**	**Permeability coefficient,Kp (cm/h) ×10-³**	**ER**
SSD-TFs-chi gel	79.38±14.26	3.44	8.12	1.92
SSD-chi gel	40.95±0.87	1.79	4.23	1.00

The cumulative permeation profiles showed a gradual increase in the amount of SSD permeated through the skin over the entire experimental period for both formulations. However, the SSD-TFs-chi gel consistently exhibited greater permeation than the SSD-chi gel, indicating the superior ability of the transfersomal system to facilitate drug transport across the skin barrier.

After 24 h, SSD-TFs-chi gel showed a cumulative permeation value (Q24) of 79.38 ± 14.26 µg/cm², whereas SSD-chi gel exhibited a significantly lower value of 40.95 ± 0.87 µg/cm². The approximately two-fold increase in permeation observed with SSD-TFs-chi gel demonstrates the effectiveness of transfersomal vesicles in improving the drug delivery across the skin.

Statistical analysis was performed using an unpaired Student's t-test, and a statistically significant difference was observed between the two formulations ($p < 0.05$),

indicating that the enhancement in permeation was attributable to the transfersomal carrier system rather than experimental variation as shown in Figure 4.10.

The permeation flux (J), obtained from the slope of the linear portion of the permeation curve, was found to be 3.44 µg/cm^2/h for SSD-TFs-chi gel compared with 1.79 µg/cm^2/h for SSD-chi gel. Similarly, the permeability coefficient (K_p) of SSD-TFs-chi gel (8.12 × 10-^{3} cm/h) was markedly greater than that of SSD-chi gel (4.23 × 10-^{3} cm/h), as shown in Table 4.7. These findings indicate that the transfersomal formulation not only increased the total amount of drug transported across the skin but also enhanced the rate of permeation. Furthermore, the enhancement ratio (ER) of 1.92 indicated that incorporating SSD into transfersomal vesicles nearly doubled permeation efficiency compared with the conventional gel formulation.

The superior permeation performance of SSD-TFs-chi gel can be explained by the unique characteristics of transfersomes, which are ultra-deformable lipid vesicles composed of phospholipids and edge activators that possess the ability to squeeze through skin pores substantially smaller than their own diameter. This flexibility allows the vesicles to penetrate the intercellular lipid domains of the skin more effectively than conventional formulations. The hydration and osmotic gradients naturally present across the skin surface further facilitate the movement of transfersomes into deeper skin layers, thereby promoting enhanced drug transport and deposition within the tissue. Previous studies have reported that the exceptional deformability of transfersomes enables them to overcome the primary barrier function of the skin and significantly improve dermal drug delivery systems [74].

Another factor contributing to the enhanced permeation is the presence of Tween 80, which served as the edge activator in the formulation. It destabilizes the phospholipid bilayer in a controlled way and increases membrane elasticity, allowing the vesicles to undergo reversible. Similar observations have been reported for tween-based transfersomal formulations, where significant increases in drug permeation and flux were attributed to enhanced vesicle flexibility and improved interaction with the skin barrier [75].

The chitosan gel matrix may also be involved in the overall permeation of the formulation. Chi is a biocompatible and bioadhesive polymer capable of maintaining prolonged contact between the formulation and the skin.

Moreover, chitosan has been reported to improve the hydration of the skin and facilitate the penetration of the drug. Recent reviews have highlighted the significant role of chitosan-based hydrogels in enhancing drug delivery and the wound healing process [76].

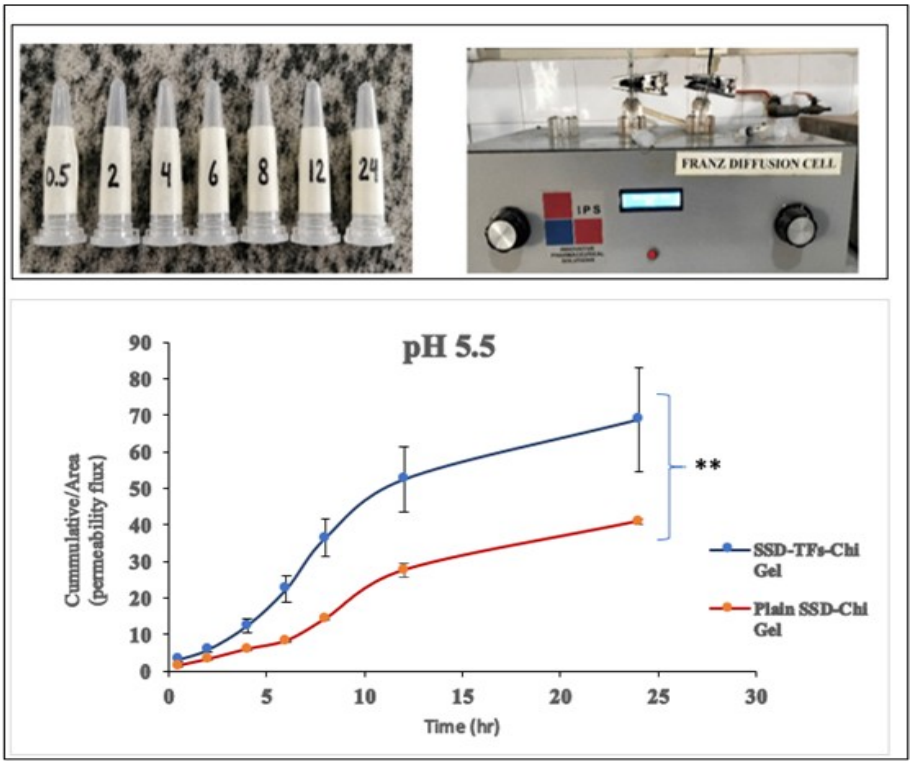

FIGURE 4.11: *Ex vivo* permeation graph of SSD-TFs-chi gel & SSD-chi gel at pH 5.5 using Franz Diffusion Cell. Results are expressed as mean ±SD (n =3). Comparisons between groups were conducted using an unpaired Student's t-test, and differences reaching* p <0.01 were considered significant when compared with plain gel

The enhanced permeation of SSD-TFs-chi gel observed in Figure 4.10 is consistent with previously reported findings for transfersomal and other vesicular systems. The higher permeation flux and permeability coefficient observed for SSD-TFs-chi gel are therefore in good agreement with the established mechanism of transfersomal transport described in the literature. The increased permeation achieved by SSD-TFs-chi gel suggests that a larger amount of SSD can reach the target

tissue, potentially improving antibacterial efficacy and accelerating the wound-healing process. In addition, the sustained permeation profile observed throughout the study indicates the potential of the transfersomal chitosan gel to provide prolonged drug release and maintain therapeutic concentrations for an extended duration.The significantly higher values of Q24, permeation flux, permeability coefficient, and enhancement ratio obtained for SSD-TFs-chi gel compared with SSD-chi gel indicate the effectiveness of the transfersomal carrier system. The primary objective of the present study was to evaluate the comparative transcutaneous transport of SSD from the optimized topical SSD-TF-Chi gel. Drug permeation was quantified in the receptor compartment using a Franz diffusion cell rather than separately quantifying SSD in the stratum corneum, epidermis, and dermis. Franz diffusion studies provide quantitative parameters such as cumulative permeation, steady-state flux, and permeability coefficient, which are appropriate for comparing the transport performance of topical formulations across the skin barrier. In contrast, layer-specific quantification is mainly required when the objective is to determine drug retention, penetration depth, or localization within specific skin layers. Therefore, the higher receptor-phase flux obtained with SSD-TF-Chi gel demonstrates enhanced transcutaneous transport of SSD compared with conventional SSD-Chi gel, but does not claim increased drug deposition in a particular skin layer. This approach is appropriate for the present formulation-development study, while layer-specific drug retention may be investigated in a subsequent dedicated study using tape stripping, sequential extraction, or imaging techniques [77].

4.8.4 Biocompatibility Studies

The dermal safety of developed SSD-TFs-chi gel was analyzed by the modified Draize skin irritation test, followed by the histopathological examination of skin sections using H&E staining. The erythema, edema, and irritation were observed at fixed times (0, 2, 4, 8, and 18 hours) following topical application of the formulations. The degree of dermal irritation was determined using the Draize scoring

system, whereby an increase in the irritation score indicates a corresponding increase in the severity of the skin response [69].

Throughout the study period, the group treated with the SSD-TFs-chi gel showed excellent dermal compatibility with no signs of erythema or edema and irritation. Thus, the formulation received a Draize score of 0, signifying a non-irritant response.

These findings indicate that both the phospholipid-based transfersomal carrier and the chitosan hydrogel matrix exhibit superior dermal compatibility and exhibit robust tolerance following topical administration. Simultaneous findings have been documented for phospholipid nanovesicular systems, where the biomimetic composition of phospholipids and mild non-ionic surfactants reduces irritation while improving interaction with the stratum corneum and enhancing topical drug delivery [69].

The histopathological examination was also performed as shown in Figure 4.12. Skin sections of the SSD-TFs-chi gel-treated group showed a normal epidermal layer, and the dermal architecture was well preserved, with normal distribution of skin appendages. No erosion of the epidermis, edema of the dermis, slight infiltration by inflammatory cells, or necrosis of the tissues was seen. The results indicated that the edge activator used with the phospholipid vesicles in the transfer system was well tolerated by the skin.

In contrast, the 2% acetic acid-treated skin exhibited the most significant histopathological variations. It demonstrated disruption of the epidermal layer associated with dense inflammatory cell infiltration, moderate dermal edema, vascular congestion, and localized degeneration of skin appendages, corresponding to moderate to severe histopathological scores. These microscopic findings are indicative of chemically induced skin irritation and exhibit a strong correlation with the positive Draize irritation response observed during visual examination. Similar pathological changes have been described in experimental irritant dermatitis models, where disruption of the epidermal barrier triggers inflammatory cell recruitment, enhanced vascular permeability, and dermal edema [78].

TABLE 4.8: All data are expressed as mean ± SD (n=3), and scoring is according to the Draize scale

Groups	**0 hr**	**2 hr**	**4 hr**	**6 hr**	**18 hr**
SSD-TFs-chl gel (test group)	E: 0 ± 0.00	E: 0 ± 0.00	E: 0 ± 0.00	E: 0 ± 0.00	E: 0 ± 0.00
	Ed: 0 ± 0.00	Ed: 0 ± 0.00	Ed: 0 ± 0.00	Ed: 0 ± 0.00	Ed: 0 ± 0.00
	I: 0 ± 0.00	I: 0 ± 0.00	I: 0 ± 0.00	I: 0 ± 0.00	I: 0 ± 0.00
2% Acetic acid (positive control)	E: 0 ± 0.00	E: 0 ± 0.00	E: 1 ± 0.00	E: 1.5 ± 0.70	E: 2.5 ± 0.70
	Ed: 0 ± 0.00	Ed: 0 ± 0.00	Ed: 1 ± 0.00	Ed: 2 ± 0.00	Ed: 2 ± 0.00
	I: 0 ± 0.00	I: 1.5 ± 0.70	I: 2.5 ± 0.70	I: 2.7 ± 0.3	I: 2.7 ± 0.3
Normal Control	E: 0 ± 0.00	E: 0 ± 0.00	E: 0 ± 0.00	E: 0 ± 0.00	E: 0 ± 0.00
	Ed: 0 ± 0.00	Ed: 0 ± 0.00	Ed: 0 ± 0.00	Ed: 0 ± 0.00	Ed: 0 ± 0.00
	I: 0 ± 0.00	I: 0 ± 0.00	I: 0 ± 0.00	I: 0 ± 0.00	I: 0 ± 0.00

E = Erythema, Ed = Edema, I = Irritation

In general, the Draize scoring and histopathological findings indicated that SSD-TFs-chi gel has good dermal biocompatibility and does not cause any skin irritation when applied topically. The lack of erythema, edema, epidermal disruption, and inflammatory infiltration indicates the safety of the developed transfersomal chitosan gel as a topical delivery system of SSD. The biocompatibility of phospholipids, the mild non-ionic surfactant system, and the protective effect of the chitosan hydrogel matrix all contribute to the reduction in skin irritation and maintenance of formulation stability and therapeutic activity [75].

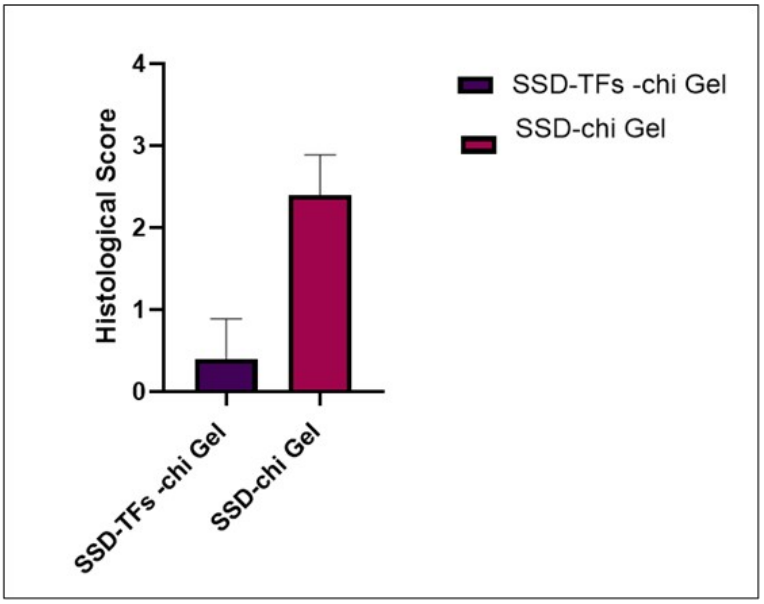

FIGURE 4.12: Morphological Histological Images of SSD-TFs-chi gel, 2% Acetic Acid Normal control

4.8.5 Stability Studies

The stability of the optimized SSD-TFs-chi gel was evaluated over six months under refrigerated (4 ± 2 °C), room temperature (25 ± 2 °C), and accelerated (40 ± 2 °C) storage conditions. The formulation remained physically stable throughout the study, with no observable colour change or loss of homogeneity under any storage condition as shown in Figure 4.10. Furthermore, no phase separation was detected during the first three months, whereas only slight phase separation was observed after six months at 25 °C and 40 °C, while the formulation stored at 4 °C remained completely stable. The pH of the formulation remained within

the physiologically acceptable range for topical application (5.38 ± 0.60 to 5.86 ± 0.05) throughout the study, indicating that neither the chitosan gel matrix nor the transfersomal vesicles underwent significant physicochemical degradation during storage. The slight pH fluctuations observed under accelerated conditions are expected because elevated temperatures increase molecular mobility and may promote limited phospholipid rearrangement or hydrolysis without substantially affecting formulation integrity.

Likewise, the minor phase separation observed at higher temperatures can be attributed to partial destabilization of the vesicular dispersion and relaxation of the polymeric gel network during prolonged storage. Similar findings have been reported for transfersomal topical gels, where refrigerated storage better preserves vesicle integrity and physicochemical characteristics than ambient or accelerated conditions [69].

Likewise, stability studies on SSD-loaded hydrogels have shown that minor physical changes may occur during accelerated storage without compromising formulation performance, provided that the pH and overall gel characteristics remain within acceptable limits [79].

TABLE 4.9: Physical Evaluation of SSD-TFs-chi gel during 6 months under different temperatures. Values are expressed as a mean ± SD(n=3)

Time	**Storage**	**Physical appearance (SSD-TFS -chi gel)**			
	Temp.	Colour change	Homogenity	Phase separation	pH
After 1 month	4 ∘C	No	No	No	5.5 ± 0.03
	25 ∘C	No	No	No	5.52 ± 0.07
	40 ∘C	No	No	No	5.57 ± 0.1
After 3 months	4 ∘C	No	No	No	5.55 ± 0.03
	25 ∘C	No	No	No	5.77 ± 0.05
	40 ∘C	No	No	No	5.75 ± 0.1

Table 4.9 continued from previous page

Time	**Storage**	**Physical appearance (SSD-TFS -chi gel)**			**pH**
	40 ∘C	No	No	No	5.44 ± 0.1
	4 ∘C	No	No	No	5.86 ±
After 6 months					0.05
	25 ∘C	No	No	Slightly	5.56 ± 0.2
	40 ∘C	No	No	Slightly	5.38 ± 0.6

Chapter 5

Conclusion and Future Recommendations

5.1 Conclusion

The present study successfully developed SSD-TFs-chi gel, providing a promising topical delivery strategy for the localized treatment of bacterial wound infections. The optimized transfersomal formulation exhibited nanosized vesicles with a well-dispersed vesicles with a narrow particle size profile, efficient incorporation of the drug, and excellent physicochemical integrity, confirming the successful incorporation of silver sulphadiazine within the phospholipid bilayer. Characterization studies using FTIR, XPRD, and FE-TEM demonstrated excellent compatibility between the drug and formulation components, preservation of the chemical integrity of silver sulphadiazine, and the formation of predominantly spherical, well-defined nanovesicles with minimal aggregation.

Following incorporation into the chitosan gel, the optimized formulation exhibited suitable physicochemical characteristics for topical application, including acceptable pH, good homogeneity, satisfactory spreadability, appropriate viscosity, and excellent physical stability under refrigerated, ambient, and accelerated storage

conditions. The formulation maintained its integrity throughout the stability assessment, the formulation retained its original appearance and remained free from phase separation, indicating satisfactory physical stability, or pH, indicating good storage stability and formulation robustness.

The in vitro drug release studies demonstrated that SSD-TFs provided significantly higher and more sustained drug release than conventional silver sulphadiazine under both pH 5.5 and pH 7.4. The enhanced release observed under mildly acidic conditions suggests that the formulation is well-suited for the wound microenvironment, where sustained local drug availability is essential for effective antimicrobial therapy. Drug release kinetic modeling further showed that the release of silver sulphadiazine from the optimized TFs was predominantly governed by diffusion-controlled mechanisms, confirming the ability of the phospholipid vesicles to regulate prolonged release of the drug over an extended duration. Ex vivo permeation studies demonstrated that encapsulation of Silver Sulphadiazine within highly deformable transfersomes significantly enhanced drug permeation compared with the conventional formulation. The flexible phospholipid vesicles facilitated efficient transport across the stratum corneum while maintaining prolonged drug retention within the skin, indicating the potential of the developed system to improve local drug delivery and therapeutic efficacy.

The optimized SSD-TFs-chi gel also exhibited superior antibacterial activity against Staphylococcus aureus, producing significantly larger zones of inhibition than conventional silver sulphadiazine. The improved antimicrobial performance is attributed to enhanced drug solubilization, sustained release, and increased interaction of the nanosized vesicles with bacterial cells, thereby providing prolonged antibacterial activity at the site of infection. Furthermore, in vivo skin irritation and histopathological evaluations confirmed the excellent dermal compatibility of the optimized formulation. The SSD-TFs-chi gel produced negligible erythema, edema, and irritation, while histological examination revealed normal epidermal and dermal architecture without evidence of inflammatory cell infiltration or tissue damage, demonstrating that the developed formulation possesses an acceptable safety profile for topical administration.

Overall, this study successfully established a stable and effective transfersomal chitosan gel platform for the topical delivery of silver sulphadiazine. The combination of enhanced drug release, improved skin permeation, sustained antibacterial activity, excellent dermal safety, and favorable physicochemical stability demonstrates that the developed formulation effectively overcomes several limitations associated with conventional silver sulphadiazine therapy. Therefore, the optimized SSD-TFs-chi gel represents a promising nanovesicular delivery system for the topical management of burn wounds and infected skin conditions and provides a strong foundation for future translational and clinical research.

5.2 Future Recommendations

The developed SSD-TFs-chi gel demonstrated promising physicochemical characteristics, sustained drug release, enhanced skin permeation, improved antibacterial activity, and excellent dermal safety. Nevertheless, additional investigations are required to facilitate its successful translation from laboratory research to clinical application. Although the present study confirmed the clinical potential of the formulated delivery system through comprehensive in vitro and ex vivo evaluations, well-designed comprehensive clinical trials involving human participants are needed to demonstrate its therapeutic efficacy, pharmacokinetic profile, long-term dermal safety, patient compliance, and overall clinical performance. Such investigations are necessary for optimizing dosage regimens and fulfilling regulatory requirements for commercialization.

Beyond SSD, the transfersomal chitosan gel platform possesses considerable versatility and offers the potential to function as a universal dermal delivery system for various hydrophobic antimicrobial and anti-inflammatory therapeutic agents and wound-healing compounds. Therapeutic agents with limited skin permeability or poor aqueous solubility may particularly benefit from incorporation into highly deformable transfersomal vesicles, thereby improving local drug availability while minimizing systemic exposure and associated adverse effects.

Considering the increasing prevalence of chronic wound infections and antimicrobial resistance, future studies should investigate the incorporation of combination antimicrobial therapies, antimicrobial peptides, natural bioactive compounds, or growth factors within the transfersomal system to achieve synergistic antibacterial activity while simultaneously promoting tissue regeneration and accelerating wound healing.

Comprehensive long-term and accelerated stability studies should be conducted according to International Council for Harmonisation (ICH) guidelines to establish the shelf life of the formulation under different environmental conditions, including variations in temperature, humidity, and light exposure. Such studies will make sure the maintenance of physicochemical stability, uniformity of drug content, microbiological quality, and therapeutic operational performance throughout storage.

The application of high-resolution imaging techniques, particularly fluorescence-based skin penetration studies, should also be employed to better understand the interaction of transfersomal vesicles with the skin barrier, their penetration pathways, intracellular transport, and drug distribution within different skin layers.

Upcoming work should also focus on evaluating the wound-healing efficacy of the optimized formulation in full-thickness burn wounds, diabetic wounds, pressure ulcers, and other chronic wound models, with a detailed assessment of wound contraction, epithelialization, collagen deposition, angiogenesis, inflammatory biomarkers, and tissue remodeling to further validate its therapeutic potential.

Comparative evaluation with marketed silver sulphadiazine formulations should also be conducted to assess the superiority of the developed transfersomal chitosan gel in terms of drug release, skin permeation, stability, wound healing efficacy, and overall comprehensive therapeutic efficacy.

Bibliography

[1] W. Żwierełło, K. Piorun, M. Skórka-Majewicz, A. Maruszewska, J. Antoniewski, and I. Gutowska, "Burns: Classification, pathophysiology, and treatment: A review," *International Journal of Molecular Sciences*, vol. 24, Feb. 2023.

[2] E. Proksch, J. M. Brandner, and J. M. Jensen, "The skin: An indispensable barrier," *Experimental Dermatology*, vol. 17, pp. 1063–1072, Dec. 2008.

[3] World Health Organization, "Burns," 2026. Accessed: 2026-02-16.

[4] J. A. D'Abbondanza and S. Shahrokhi, "Burn infection and burn sepsis," *Surgical Infections*, vol. 22, pp. 58–64, Feb. 2021.

[5] Y. Cho, C. Seo, and S. Joo, "Burn injury," *Burns & Trauma*, 2020.

[6] M. G. Jeschke, M. E. van Baar, M. A. Choudhry, K. K. Chung, N. S. Gibran, and S. Logsetty, "Burn injury," *Nature Reviews Disease Primers*, vol. 6, Feb. 2020.

[7] D. G. Greenhalgh, "Management of burns," *New England Journal of Medicine*, vol. 380, pp. 2349–2359, June 2019.

[8] W. S. Siu, H. Ma, and P. C. Leung, "Review on current advancements in facilitation of burn wound healing," *Bioengineering*, vol. 12, p. 428, Apr. 2025.

[9] E. J. Kelly, M. A. Oliver, B. C. Carney, and J. W. Shupp, "Infection and burn injury," *European Burn Journal*, vol. 3, pp. 165–179, Mar. 2022.

[10] E. M. Tottoli, R. Dorati, I. Genta, E. Chiesa, S. Pisani, and B. Conti, "Skin wound healing process and new emerging technologies for skin wound care and regeneration," *Pharmaceutics*, vol. 12, p. 735, Aug. 2020.

[11] T. Guiddir *et al.*, "Unusual initial abdominal presentations of invasive meningococcal disease," *Clinical Infectious Diseases*, vol. 67, pp. 1220–1227, Sept. 2018.

[12] J. Maitz, J. Merlino, S. Rizzo, G. McKew, and P. Maitz, "Burn wound infections microbiome and novel approaches using therapeutic microorganisms in burn wound infection control," *Advanced Drug Delivery Reviews*, vol. 196, p. 114769, May 2023.

[13] H. A. Ladhani, C. J. Yowler, and J. A. Claridge, "Burn wound colonization, infection, and sepsis," *Surgical Infections*, vol. 22, pp. 44–48, Feb. 2021.

[14] Y. Wang *et al.*, "Burn injury: Challenges and advances in burn wound healing, infection, pain and scarring," *Advanced Drug Delivery Reviews*, vol. 123, pp. 3–17, Jan. 2018.

[15] D. R. Alves *et al.*, "Development of a high-throughput ex-vivo burn wound model using porcine skin, and its application to evaluate new approaches to control wound infection," *Frontiers in Cellular and Infection Microbiology*, vol. 8, p. 196, June 2018.

[16] X. Liu *et al.*, "Combined silver sulfadiazine nanosuspension with thermosensitive hydrogel: An effective antibacterial treatment for wound healing in an animal model," *International Journal of Nanomedicine*, vol. 18, pp. 679–691, 2023.

[17] D. Monti, S. Tampucci, R. Tiwari, and K. Pathak, "Local drug delivery strategies towards wound healing," *Pharmaceutics*, vol. 15, p. 634, Feb. 2023.

[18] J. A. G. Garcia, A. M. G. Chavez, and J. D. J. O. Grados, "Topical antimicrobial agents for the prevention of burn-wound infection. what do international guidelines recommend? a systematic review," *World Journal of Plastic Surgery*, vol. 11, p. 3, Aug. 2022.

[19] S. Razavi, A. Partoazar, N. Takzaree, M. Fasihi-Ramandi, A. Bahador, and M. H. Darvishi, "Silver sulfadiazine nanoethogel for burn healing: Characterization and investigation of its in vivo effects," *Nanomedicine*, vol. 13, no. 11, pp. 1319–1331, 2018.

[20] G. S. El-Feky, S. T. El-Banna, G. El-Bahy, E. Abdelrazek, and M. Kamal, "Alginate coated chitosan nanogel for the controlled topical delivery of silver sulfadiazine," *Carbohydrate Polymers*, vol. 177, pp. 194–202, 2017.

[21] B. S. Atiyeh, S. A. Dibo, and S. N. Hayek, "Wound cleansing, topical antiseptics and wound healing," *International Wound Journal*, vol. 6, pp. 420–430, Dec. 2009.

[22] R. Fernández-García, A. Lalatsa, L. Statts, F. Bolás-Fernández, M. P. Ballesteros, and D. R. Serrano, "Transferosomes as nanocarriers for drugs across the skin: Quality by design from lab to industrial scale," *International Journal of Pharmaceutics*, vol. 573, p. 118817, Jan. 2020.

[23] M. A. Kassem, M. H. Aboul-Einien, and M. M. E. Taweel, "Dry gel containing optimized felodipine-loaded transferosomes: A promising transdermal delivery system to enhance drug bioavailability," *AAPS PharmSciTech*, vol. 19, no. 5, pp. 2155–2173, 2018.

[24] S. Taymouri, V. Hajhashemi, M. Tabbakhian, and M. Torkashvand, "Preparation and evaluation of imatinib loaded transfersomal gel for the treatment of rheumatoid arthritis," *Iranian Journal of Pharmaceutical Research*, vol. 20, pp. 33–49, Oct. 2021.

[25] S. Batool *et al.*, "Macrophage targeting with the novel carbopol-based miltefosine-loaded transfersomal gel for the treatment of cutaneous leishmaniasis: In vitro and in vivo analyses," *Drug Development and Industrial Pharmacy*, vol. 47, no. 3, pp. 440–453, 2021.

[26] S. Bhattacharyya *et al.*, "Formulation and evaluation of a transferosomal gel of famciclovir for transdermal use," *Turkish Journal of Pharmaceutical Sciences*, vol. 21, pp. 303–312, Aug. 2024.

[27] R. Z. Khattak *et al.*, "Formulation, in vitro characterization and antibacterial activity of chitosan-decorated cream containing bacitracin for topical delivery," *Antibiotics*, vol. 11, p. 1151, Aug. 2022.

[28] A. Pandey, M. Momin, and A. Chando, "Silver sulfadiazine loaded breathable hydrogel sponge for wound healing," *Drug Metabolism and Personalized Therapy*, vol. 35, Sept. 2020.

[29] E. A. Gantwerker and D. B. Hom, *Physiology, Wound Healing*. Treasure Island, FL: StatPearls Publishing, 2025.

[30] International Wound Infection Institute, "Wound infection continuum: Consensus update," 2016. Consensus document.

[31] Physiopedia, "Assessment of wound infection." https://www.physio-pedia.com/Assessment_of_Wound_Infection, 2026. Accessed: 2026-02-26.

[32] F. D. Francesco, M. Riccio, and S. Jimi, "Contribution of topical agents such as hyaluronic acid and silver sulfadiazine to wound healing and management of bacterial biofilm," *Medicina*, vol. 58, p. 835, June 2022.

[33] H. Barkat, M. A. Barkat, R. Ali, and H. Hadi, "Nanotechnological advances in burn wound care: Silver sulfadiazine-loaded nanosuspension-based chitosan-incorporated nanogel for partial thickness burns," *Journal of Burn Care & Research*, 2025.

[34] J. Zhou *et al.*, "Thermosensitive black phosphorus hydrogel loaded with silver sulfadiazine promotes skin wound healing," *Journal of Nanobiotechnology*, vol. 21, Dec. 2023.

[35] L. Lopez-Vidal *et al.*, "Advanced drug delivery systems for the management of local conditions," *Therapeutic Delivery*, vol. 16, no. 3, pp. 285–303, 2025.

[36] W. Wang, K. J. Lu, C. H. Yu, Q. L. Huang, and Y. Z. Du, "Nano-drug delivery systems in wound treatment and skin regeneration," *Journal of Nanobiotechnology*, vol. 17, p. 82, July 2019.

[37] N. Matharoo, H. Mohd, and B. Michniak-Kohn, "Transferosomes as a transdermal drug delivery system: Dermal kinetics and recent developments," *WIREs Nanomedicine and Nanobiotechnology*, vol. 16, p. e1918, Jan. 2024.

[38] K. S. N. L. G. A. P. A. G. Raj, V. Shabna, S. A. M, *et al.*, "Transferosomes, revolutionizing nsaids delivery for improved therapeutic efficacy: A systematic review of formulation strategies and evaluations," *International Journal of Pharmaceutical Sciences*, vol. 2, no. 8, pp. 3553–3560, 2024.

[39] J. L. do Nascimento *et al.*, "Laponite®-based smart hydrogels for sustained topical delivery of silver sulfadiazine: A strategy for the treatment of contaminated or biofilm-forming wounds," *Pharmaceutics*, vol. 17, Sept. 2025.

[40] N. B. Mutlu-Ağardan, S. Tort, Ş. Aydoğduoğlu, and M. E. Kıymacı, "A new insight to silver sulfadiazine antibacterial dressings: Nanoparticle-loaded nanofibers for controlled drug delivery," *AAPS PharmSciTech*, vol. 24, Jan. 2023.

[41] T. Luo *et al.*, "Co-delivery of superfine nano-silver and solubilized sulfadiazine for enhanced antibacterial functions," *International Journal of Pharmaceutics*, vol. 584, June 2020.

[42] X. Liu *et al.*, "Silver sulfadiazine nanosuspension-loaded thermosensitive hydrogel as a topical antibacterial agent," *International Journal of Nanomedicine*, vol. 14, pp. 289–300, 2019.

[43] M. A. S. Al-Janabi and S. S. N. Al-Edresi, "Preparation and validation of nanofibers loaded with silver sulfadiazine from zein/poly(ε-caprolactone)/poly(ethylene oxide) for topical dosage forms to improve release behaviour," *Journal of Research in Pharmacy*, vol. 28, pp. 2114–2125, June 2025.

[44] M. A. Barkat *et al.*, "Nanosuspension-based aloe vera gel of silver sulfadiazine with improved wound healing activity," *AAPS PharmSciTech*, vol. 18, pp. 3274–3285, Nov. 2017.

[45] H. Razavi, M. H. Darvishi, and S. Janfaza, "Silver sulfadiazine encapsulated in lipid-based nanocarriers for burn treatment," *Journal of Burn Care & Research*, vol. 39, pp. 319–325, Apr. 2018.

[46] M. Venkataraman and M. Nagarsenker, "Silver sulfadiazine nanosystems for burn therapy," *AAPS PharmSciTech*, vol. 14, no. 1, pp. 254–264, 2013.

[47] G. S. El-Feky, S. S. Sharaf, A. E. Shafei, and A. A. Hegazy, "Using chitosan nanoparticles as drug carriers for the development of a silver sulfadiazine wound dressing," *Carbohydrate Polymers*, vol. 158, pp. 11–19, Feb. 2017.

[48] V. S. Mastiholimath, C. T. W. Valerie, V. S. Mannur, P. M. Dandagi, A. P. Gadad, and P. Khanal, "Formulation and evaluation of solid lipid nanoparticle containing silver sulfadiazine for second and third degree burn wounds and its suitable analytical method development and validation," *Indian Journal of Pharmaceutical Education and Research*, vol. 54, pp. 31–45, Jan. 2020.

[49] K. Ito *et al.*, "Sustainable antimicrobial effect of silver sulfadiazine-loaded nanosheets on infection in a mouse model of partial-thickness burn injury," *Acta Biomaterialia*, vol. 24, pp. 87–95, Sept. 2015.

[50] M. Waqas *et al.*, "Silver sulfadiazine loaded nanofibers for burn infections," *International Journal of Polymeric Materials and Polymeric Biomaterials*, vol. 72, no. 7, pp. 517–523, 2023.

[51] N. M. Morsi, G. A. Abdelbary, and M. A. Ahmed, "Silver sulfadiazine based cubosome hydrogels for topical treatment of burns: Development and in vitro/in vivo characterization," *European Journal of Pharmaceutics and Biopharmaceutics*, vol. 86, pp. 178–189, Feb. 2014.

[52] Pakistan Journal of Ophthalmology, "Evaluation of chitosan; a thermosensitive hydrogel drug delivery agent for loading dexamethasone," 2026. Accessed: 2026-04-21.

[53] S. Peers, A. Montembault, and C. Ladavière, "Chitosan hydrogels for sustained drug delivery," *Journal of Controlled Release*, vol. 326, pp. 150–163, Oct. 2020.

[54] A. S. Fard, Z. Sabouri, M. Darroudi, and R. Arezumand, "Application of chitosan-based nanogels for dermal and transdermal delivery systems," *Journal of Materials Science: Materials in Medicine*, vol. 37, no. 1, 2025.

[55] A. Salahuddin, A. Ashraf, K. Ahmad, and H. Hou, "Recent advances in chitosan-based smart hydrogel for drug delivery systems," *International Journal of Biological Macromolecules*, vol. 280, p. 135803, Nov. 2024.

[56] T. Kazim, A. Tariq, M. Usman, M. F. Ayoob, and A. Khan, "Chitosan hydrogel for topical delivery of ebastine loaded solid lipid nanoparticles for alleviation of allergic contact dermatitis," *RSC Advances*, vol. 11, pp. 37413–37425, Nov. 2021.

[57] L. Zhang, Z. Yu, D. Wang, Y. Shang, Y. Y. Liu, and H. W. Zhang, "Chitosan-based infected wound care: A bibliometric analysis from 2002 to 2025," *Medicine*, 2026. Advance online publication.

[58] S. Alven and B. A. Aderibigbe, "Chitosan-based scaffolds incorporated with silver nanoparticles for the treatment of infected wounds," *Pharmaceutics*, vol. 16, p. 327, Feb. 2024.

[59] E. Sana *et al.*, "Topical delivery of curcumin-loaded transfersomes gel ameliorated rheumatoid arthritis by inhibiting nf-κb pathway," *Nanomedicine*, vol. 16, pp. 819–837, Apr. 2021.

[60] H. M. Tawfeek, A. A. H. Abdellatif, J. A. Abdel-Aleem, Y. A. Hassan, and D. Fathalla, "Transfersomal gel nanocarriers for enhancement the permeation of lornoxicam," *Journal of Drug Delivery Science and Technology*, vol. 56, Apr. 2020.

[61] G. F. Balata, M. M. Faisal, H. A. Elghamry, and S. A. Sabry, "Preparation and characterization of ivabradine hcl transfersomes for enhanced transdermal delivery," *Journal of Drug Delivery Science and Technology*, vol. 60, Dec. 2020.

[62] N. Joshi, N. Mishra, and V. K. Rai, "Development and evaluation of in situ gel of silver sulfadiazine for improved therapeutic efficacy against infectious burn wound," *Journal of Pharmaceutical Innovation*, vol. 16, pp. 537–550, Sept. 2021.

[63] M. Rosmiati, M. Abdassah, and A. Y. Chaerunisaa, "Effect of carrageenan as gelling agent on tocopherol acetate emulgels," *Indonesian Journal of Pharmaceutical Science and Technology*, vol. 5, no. 1, pp. 1–7, 2018.

[64] C. Upadhyay, Vibha, D. Pathak, and M. Kulshreshtha, "Preparation and evaluation of different herbal gels synthesized from chinese medicinal plants as antimicrobial agents," *Pharmacological Research – Modern Chinese Medicine*, vol. 9, Dec. 2023.

[65] R. Klopfleisch, "Multiparametric and semiquantitative scoring systems for the evaluation of mouse model histopathology – a systematic review," *BMC Veterinary Research*, vol. 9, p. 123, June 2013.

[66] Z. F, R. R, and S. K, "A review on stability testing guidelines of pharmaceutical products," *Asian Journal of Pharmaceutical and Clinical Research*, pp. 3–9, Aug. 2020.

[67] M. M. A. Elsayed *et al.*, "Deformable liposomes and ethosomes as carriers for skin delivery of ketotifen," *Die Pharmazie*, vol. 62, pp. 133–137, Feb. 2007.

[68] M. W. Akram, H. Jamshaid, F. U. Rehman, M. Zaeem, J. Z. Khan, and A. Zeb, "Transfersomes: A revolutionary nanosystem for efficient transdermal drug delivery," *AAPS PharmSciTech*, vol. 23, Jan. 2022.

[69] S. A. T. Opatha, V. Titapiwatanakun, and R. Chutoprapat, "Transfersomes: A promising nanoencapsulation technique for transdermal drug delivery," *Pharmaceutics*, vol. 12, p. 855, Sept. 2020.

[70] R. Squittieri, L. Baldino, and E. Reverchon, "Production of antioxidant transfersomes by a supercritical co_2 assisted process for transdermal delivery applications," *Nanomaterials*, vol. 13, p. 1812, June 2023.

[71] R. Batool, S. Ayub, and I. Akbar, "Isolation of biosurfactant producing bacteria from petroleum contaminated sites and their characterization," *Soil and Environment*, vol. 36, no. 1, pp. 35–44, 2017.

[72] M. I. Khan *et al.*, "Development and in vitro/ex vivo evaluation of lecithin-based deformable transfersomes and transfersome-based gels for combined dermal delivery of meloxicam and dexamethasone," *BioMed Research International*, vol. 2022, p. 8170318, 2022.

[73] S. Jain, P. Jain, R. B. Umamaheshwari, and N. K. Jain, "Transfersomes–a novel vesicular carrier for enhanced transdermal delivery: Development, characterization, and performance evaluation," *Drug Development and Industrial Pharmacy*, vol. 29, no. 9, pp. 1013–1026, 2003.

[74] B. Dixena, R. Madhariya, A. Panday, A. Ram, and A. K. Jain, "Overcoming skin barrier with transfersomes: Opportunities, challenges, and applications," *Current Drug Delivery*, vol. 22, pp. 160–180, Jan. 2025.

[75] H. A. Hadi and A. H. Hussein, "Comparison study between tween 20 and tween 80 as an edge activator for preparation of transdermal ondansetron hcl transfersomal nano particles," *Journal of Population Therapeutics and Clinical Pharmacology*, vol. 30, pp. 164–180, Feb. 2023.

[76] N. Yuan, K. Shao, S. Huang, and C. Chen, "Chitosan, alginate, hyaluronic acid and other novel multifunctional hydrogel dressings for wound healing: A review," *International Journal of Biological Macromolecules*, vol. 240, p. 124321, June 2023.

[77] S. Chaturvedi and A. Garg, "An insight of techniques for the assessment of permeation flux across the skin for optimization of topical and transdermal drug delivery systems," *Journal of Drug Delivery Science and Technology*, vol. 62, p. 102355, 2021.

[78] N. M. Malewicz-Oeck, Z. Zhang, S. G. Shimada, and R. H. LaMotte, "Itch and pain behaviors in irritant contact dermatitis produced by sodium lauryl

sulfate in mice," *International Journal of Molecular Sciences*, vol. 25, p. 7718, July 2024.

[79] L. V. Vaz *et al.*, "Development and characterization of a hydrogel containing silver sulfadiazine for antimicrobial topical applications. part ii: Stability, cytotoxicity and silver release patterns," *Brazilian Journal of Pharmaceutical Sciences*, vol. 58, 2022.